

UTRECHT UNIVERSITY

EARTH SURFACE & WATER

COASTAL DYNAMICS & FLUVIAL SYSTEMS

Bend sorting of bed load in a rotating annular flume

Author:

Steven A.H. WEISSCHER

Supervisors:

Prof. Dr. Maarten G. KLEINHANS

Anne W. BAAR, MSc.

Final version

28th January 2017

Bend sorting of bed load in a rotating
annular flume
S.A.H. Weisscher
Student number: 3901351

Supervisors
prof. dr. M.G. Kleinhans
A.W. Baar MSc.

Utrecht University
Faculty of Geosciences
Department of Physical Geography

Earth Surface & Water
Coastal Dynamics & Fluvial Systems

In cooperation with
Delft University of Technology

Final version, 28th January 2017

Universiteit Utrecht



TU Delft Delft
University of
Technology

Abstract

River bends are characterised by a transversely sloped bed profile, which is steepest in the outer bend (thalweg) and shallowest in the inner bend (point bar). Sediment, consisting of a range of grain sizes, is sorted laterally by bend flow and the transverse bed slope effect, and vertically by bed forms. It is unclear however how the degree of bend (=lateral) sorting is related quantitatively to these processes; field data and experimental research on this matter are limited, and the effects on and of sorting are not well captured in current fluvial numerical models. Therefore, it is the objective of this study to examine the effect of transverse bed slope and sediment mobility on the degree of bend sorting in a meander.

To this end, a near-unimodal sediment mixture ($d_{50,in} = 0.75$ mm) was used in a rotating annular flume. A rotating lid steers the flow and counter-rotation of the flume itself generates a centrifugal force on the flow low in the water column, weakening secondary flow intensity. By varying the rotation speeds of the lid and flume, the effect of the transverse bed slope and sediment mobility were isolated.

Two sets of experiments were conducted: sorting experiments and morphology experiments. The former were experiments of which the bed resembled natural river morphology best, namely aimed at transverse slopes between 0 and 0.25. Digital elevation models were generated for both sets, and only the sorting experiments were analysed in further detail, involving taking photographs and sediment samples.

Bend sorting becomes more distinct with steeper transverse slope. Especially slopes over 0.15 show well developed bend sorting. Sediment mobility has an insignificant effect on the sorting process as long as all sediment is transported as bed load. Only at or just below the threshold of motion is sediment mobility hypothesised to influence lateral sorting; hiding and exposure effects become prominent and a lag layer in the outer bend may form.

Longitudinal variation in bend sorting is observed on the bed form length scale. This is caused by dunes acting as obstacles of flow, leading to high secondary flow intensity, and therefore steep slopes, in the dune troughs. Also, dunes sort sediment vertically that is made available by lateral sorting, in a fining upward trend.

On the natural river scale, most pronounced bend sorting is expected in sand bed rivers with high sinuosity (predominantly meandering and sinuous rivers). Least pronounced sorting is expected in mixed sand-gravel bed and gravel bed rivers, especially in case of threshold channels.

Hiding and exposure effects were mitigated in this study, but are argued to influence the transverse slope development and bend sorting. Elaboration on the annular flume experiments with wide sediment mixtures and field campaigns in mixed sand-gravel bed rivers are proposed.

Keywords River bend, bend sorting, bed load, transverse bed slope, secondary flow, sediment mobility, experiment, annular flume.

抄録

湾曲流路の横断斜面の外側は一番深く、内側では一番浅い。混合砂の横断的分布には、砂粒子に作用する重力と二次流の比が影響し、混合砂の縦断的分布には砂床形が影響する。実河川データと、実験結果が乏しいことに加え、混合砂の分布の影響は数値計算モデルに十分に組み込まれていないため、円形回転水路で、混合砂の流動性と、混合砂からなる横断斜面の影響を調べるのが今研究の目的である。

単峰型の粒度分布を待つ砂の中央粒径は $d_{50,in} = 0.75 \text{ mm}$ である。円形回転水路により、混合砂の流動性と、混合砂からなる横断斜面の影響は隔てられる。

二組の実験が使われる。実際の河川形態に最も近い1回目の実験では、横断分布サンプルを取り、写真を撮った。2回目の実験では、写真だけ撮った。さらに、デジタル標高モデルを作成した。

混合粒砂の横断分布は湾曲流路の急勾配のときに際立ち、とりわけ0.15より大きな勾配で顕著である。また、砂の流動性は重要ではない。混合粒砂の横断分布は、縦方向に砂床形の長さ目盛に違う。水流を阻害する砂丘は急な二次流を引き起こす。したがって砂丘の谷の部分には急な傾斜が生じる。

実河川において、河床が砂で埋まっている曲がりくねった河川が最も明瞭な横断分布を見込むことができ、河低が砂利で埋まっている河川は横断分布が最も不明瞭になると見込まれる。混合砂の流動性の違いは横断斜面の形成と混合流砂の横断分布に影響すると考えられるが、本研究では考慮されていない。混合砂の比率を変えての追加実験と、現地調査を提案する。

Contents

Abstract	iii
抄録 (in Japanese)	v
1 Introduction	1
1.1 Problem description	1
1.2 Objective of this study	1
1.3 Outline thesis	2
2 Literature review	3
2.1 Secondary flow in river bends	3
2.2 Transverse bed slope effect	6
2.3 Deviation angle of bed load transport	7
2.4 Sediment sorting in river bends	10
2.4.1 Lateral: bend sorting	10
2.4.2 Vertical: sorting by bed forms	15
2.5 Effect of bed forms on the slope factor β	17
2.6 Flume types used in previous research	18
2.6.1 Straight flumes	18
2.6.2 Curved flumes	18
2.6.3 Rotating annular flumes	19
2.7 Gaps in knowledge	20
2.8 Hypotheses	20
3 Materials & methods	21
3.1 Experimental setup	21
3.2 Experimental conditions	23
3.3 Data acquisition and processing	24
4 Results	27
4.1 Qualitative description of the experiments	28
4.2 Lateral sorting	32
4.2.1 Effect of transverse bed slope	32
4.2.2 Effect of sediment mobility	36
4.3 Bed forms in the carousel flume	37
5 Discussion	39
5.1 Bend sorting in an annular flume	39
5.1.1 Effect of the transverse slope	40
5.1.2 Effect of sediment mobility	41
5.1.3 Effect of lateral sorting on the bed form regime	42
5.2 Implications for natural rivers	43
6 Conclusions	45

7 Future research	47
7.1 Hiding and exposure effects	47
7.2 Corkscrew currents due to skewed dunes	47
Acknowledgements	49
References	51
Nomenclature	55
Appendices	57
A Notes on samples of all sorting experiments	57

List of Figures

1.1	Spatial distribution of median grain size near the bifurcation at Pannerden’s Head (NL).	2
2.1	Deflection of sediment on a transversely inclined slope	6
2.2	Transverse slope range of natural rivers.	8
2.3	Vertically averaged flow in a) an idealised and b) a natural river bend.	10
2.4	Bed load transport vectors for three mass percentile fractions of the bulk sediment over the channel width in a natural meander.	11
2.5	Sorting on and along point bars of the Allier.	11
2.6	Lateral sorting in two experimental studies, both using a curved flume.	12
2.7	Transverse bed development and bend sorting in a 180° degree flume bend.	13
2.8	Three-phase-process of sediment deposition and sorting on lee slopes of experimental deltas, analogous to dunes, that leads to fining upward.	15
2.9	Schematic cross-section of a bed levelling experiment in a straight flume, starting with an initial sinuous transverse slope.	18
3.1	Experimental setup: the Cees Kranenburg carousel flume.	21
3.2	Schematic representation of sampling and scanned bed elevation radii.	24
3.3	Grain size distribution of the sediment mixture used in this study.	25
4.1	Overview of measured transverse bed slopes for all experiments.	27
4.2	Initial bed forms that travelled oblique to the streamwise flow toward the inner bend.	28
4.3	Transverse bed slope development.	29
4.4	Impression of morphology and grain size distribution on a near-horizontal transverse bed.	29
4.5	Ripples and sheet ripples in the annular flume.	30
4.6	Well developed bend sorting on the lee side of a dune in an experiment with a steep transverse slope.	30
4.7	Digital elevation models and mean transverse slopes for corners of the measured reach $\partial z_b/\partial n$ and θ/θ_{cr}	31
4.8	Effect of increasing transverse bed slope on lateral sorting.	32
4.9	Effect of transverse bed slope on lateral sorting, split into three classes: near-horizontal slopes, mild slopes and steep slopes.	33
4.10	Standard deviation versus median grain size for the entire data set.	34
4.11	Skewness versus median grain size for the entire data set.	35
4.12	Effect of sediment mobility on bend sorting for steep transverse slopes.	36
4.13	Bed form shift over the lateral, shown in the bed form diagram.	37
4.14	Dune height dependence on secondary flow intensity.	38
4.15	Fining upward trends in the inner and outer bend for a steep and gentle transverse slope.	38
5.1	Lateral sorting described as $d_{50}/d_{50,in} = a \cdot (r/r_c)^b$ for a) near-horizontal slopes, b) mild slopes and c) steep slopes for the top, trough and bulk samples.	39
5.2	Coefficients a and b in eq. 2.17 as function of transverse slope for the dune tops.	40

5.3	Comparison with earlier studies, all showing a net decrease of the slope factor with larger non dimensionalised bed shear stress.	42
5.4	Fairly sharp river bend in braided river network, Rakaia River (NZ).	43

List of Tables

2.1	Expressions for parameter K , that determines the deviation of bed shear stress due to secondary flow.	5
2.2	Expressions for the slope parameter.	9
4.1	Flow and morphology-related parameters for the sorting experiments.	27
4.2	Internal variability of lateral sorting.	33

1 Introduction

1.1 Problem description

Fluvial systems consist of alluring channel and bar patterns, which are of great socioeconomic and ecological value. Such patterns arise from sediment transport nonlinearity, that is, sediment transport responds to flow velocity to a power greater than one (e.g. Meyer-Peter and Mueller, 1948; Van Rijn, 1984a). So, channels have a tendency to deepen. This is counterbalanced by lateral pull-down of sediment by gravity on transverse bed slopes (Van Bendegom, 1947). In meanders, there is a second lateral force that acts on the grains, namely secondary flow, which is generated as water flows along a bend. This secondary current transports sediment to the inner bend, thus acting in opposing direction to the gravitational pull-down (Van Bendegom, 1947; Sekine and Parker, 1992). The resultant transverse slope lies between 0 and 0.30 in natural meanders (e.g. Rozowskii, 1961; Jackson, 1975; Dietrich and Smith, 1983; Thorne et al., 1985; Odgaard 1981; 1987; Julien and Anthony, 2002; Clayton and Pitlick, 2007).

Previous research focused mainly on the development of the transverse bed slope using uniform sediment (e.g. Ikeda, 1982; Struiksmā et al., 1985; Talmon et al., 1995). Accordingly, spatial sorting was absent. However, spatial sorting is observed in natural meanders, both in lateral and longitudinal direction (e.g. Dietrich and Smith, 1983; Julien and Anthony, 2002; Clayton and Pitlick, 2007); coarser grains are predominantly found in the outer bend while the inner bend is fairly fine-grained. Furthermore, Ikeda et al. (1987) argued that there is a feedback mechanism between lateral sorting and the transverse bed slope, the latter of which influences e.g. braiding intensity and active channel width.

When such lateral sorting establishes just upstream of a bifurcation due to the presence of a bend, it strongly influences the distribution of grain sizes over the two downstream branches. For example at the 'Pannerdensche Kop' (Pannerden's Head) in the Netherlands, where one of the downstream branches (Pannerden Canal) is significantly coarser than the other (Waal River) (Figure 1.1) (Gruijters et al., 2001; Sloff and Mosselman, 2012). And since the transverse slope is grain size dependent, this divergence of grain size may influence the fluvial pattern of the downstream branches.

So, there is a demand for better understanding of how sorting in a river bend comes about, which can be attained by means of thorough field research, numerical modelling and scaled experiments.

1.2 Objective of this study

Natural rivers are complex systems which pose considerable difficulties when studying spatial sorting; parameters such as secondary flow intensity, sediment mobility and the grain size distribution are unmodifiable. Numerical models are great tools to provide insight and test hypotheses, but require simplifications and assumptions (Oreskes et al., 1994), in this case related to the processes that govern spatial sorting in meanders, which are still poorly understood. Repeatedly tweaking parameters that are believed to influence these processes in order to attain a desired result that resembles natural rivers, does not necessarily lead to better understanding of the process itself.

In this study, an experimental approach was chosen, which allows the study of spatial sorting in meanders in a simplified, controllable manner on a small scale, where the effect of

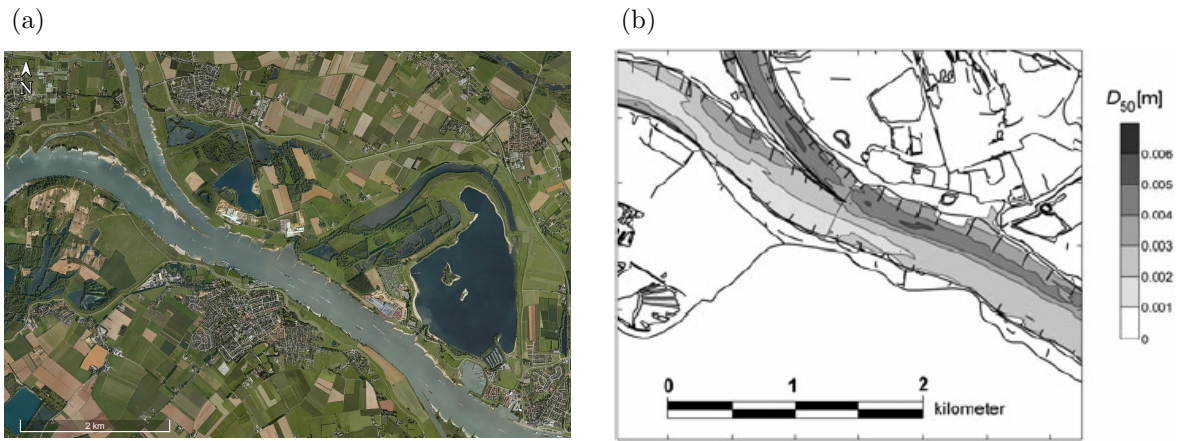


Figure 1.1: a) Bifurcation at Pannerden's Head (Google Earth imagery, accessed January 2016).
 b) Spatial distribution of median grain size near the Pannerden's Head, based on sediment sampling by [Gruijters et al. \(2001\)](#) (in [Sloff and Mosselman, 2012](#)).

different variables on sorting can be isolated. This is also a drawback of experiments: boundary and initial conditions are simplified and one has to deal with scale effects.

To make a first assessment, this study looks into how lateral sorting depends on two key parameters, namely: the steepness of the transverse slope and the mobility of bed load sediment. The latter is often assumed to be the sole parameter that influences the deviation of sediment transport with respect to streamwise flow, for a given transverse slope and secondary flow intensity (e.g. [Engelund, 1981](#); [Struiksmma et al., 1985](#)). Furthermore, new insights can be used to estimate where along a bend and in what river types well developed lateral sorting occurs.

So, the main objective of this study is:

- to determine the effect of the transverse bed slope and sediment mobility on the degree of lateral sorting in a river bend.

1.3 Outline thesis

First, a theoretical background is given on current understanding of lateral and vertical sorting in river bends and how this was studied in previous experimental studies in chapter 2. Based on this, hypotheses are formulated that were tested in an annular flume. Next, the experimental setup, conditions and data acquisition are explained in chapter 3. This is followed by the results in chapter 4. In chapter 5, the results are discussed, based on which it is debated in what kind of rivers well developed bend sorting may form. Finally, the conclusions are presented (chapter 6).

2 Literature review

In this chapter, the theoretical framework for sediment sorting in river bends is described. First, the two lateral forces acting on grains on a transverse bed slope are discussed separately, namely secondary flow and gravity. Next, combination of these forces leads to the deviation angle of bed load transport on transverse slopes. This is followed by current understanding of lateral and vertical sorting in meanders. Subsequently, the use and (dis)advantages of three types of flumes are described that were used in this field of expertise. Finally, the hypotheses are stated.

2.1 Secondary flow in river bends

Natural rivers are somewhere between straight, meandering and braided (e.g. [Leopold and Wolman, 1957](#); [Kleinhans and Van den Berg, 2011](#)), and are an important means of transporting water and sediment to lower-lying areas and oceans. Regardless of river type, practically all rivers have bends: either weak and infrequent in case of straight rivers or sharp and strongly repetitive in case of meandering and sinuous rivers.

When water flows along a bend, lateral forces come into existence to allow the flow to turn. Accordingly, a secondary, circular current is generated perpendicular to the streamwise flow ([Van Bendegom, 1947](#)). On the one hand, it reorganises momentum of the flow, causing flow to focus on the outer bend. Therefore, highest flow velocities are expected near the outer bend. On the other hand, the secondary current brings about a transverse bed shear stress component toward the inner bend ([Van Bendegom, 1947](#); [Engelund, 1974](#)). Generally, secondary flow is an order of magnitude smaller than the mean current.

To understand how secondary flow comes about and how it can be approximated physically, first steady uniform flow in a rectangular channel is considered. Given the channel is wide and has a large radius compared to its depth, and focusing only on the middle reach of the channel where vertical velocities are negligible, the following force balance holds ([Engelund, 1974](#)):

$$-\frac{u_{s,z}^2}{r} = -\frac{\partial}{\partial r}(gh) + \varepsilon \frac{\partial^2 u_n}{\partial z^2} \quad (2.1)$$

in which u is maximum local flow velocity decomposed in streamwise (s) and transverse (n) direction, z is the vertical coordinate, positive downward, r is the local radius of channel curvature, g is a gravitational constant, h is the local water depth, and ε is the eddy viscosity given as a function of shear velocity u_* :

$$\varepsilon = 0.077u_*h \quad (2.2)$$

The left-hand side of eq. 2.1 describes the centrifugal force per unit mass that a parcel of water is subjected to ([Engelund, 1974](#)). This causes superelevation of the water level in the outer bend. In consequence, a constant pressure gradient is generated in opposing direction, given as the first term on the right-hand side of eq. 2.1. Because $u_{s,z}$ varies over the water column, the depth-dependent centrifugal force cannot be compensated by a constant pressure head alone. Therefore, a friction term is required, which is the second term on the right-hand side of eq. 2.1.

Bottom and air friction cause variation of $u_{s,z}$ over the water column. Near the bed, flow velocity approaches zero while near the water surface it reaches its maximum. For turbulent

flow, this trend can be described by

$$u_{s,z} = \frac{u_*}{\kappa} \ln \frac{h_z}{z_0} \quad (2.3)$$

with

$$u_* = \sqrt{\tau/\rho} \quad (2.4)$$

where κ is the Von Karman's constant (~ 0.4), z_0 is the roughness height, ρ is water density and τ is the total bed shear stress (including bed form friction), given as

$$\tau = \rho g R_h \sin S \quad (2.5)$$

in which R_h is the hydraulic radius and S is the maximum local water surface slope. Total bed shear stress can also be described as function of the Chezy parameter C :

$$\tau = \rho g \frac{u^2}{C^2} \quad (2.6)$$

with

$$C = 18 \log_{10} \frac{12R_h}{k_s} \quad (2.7)$$

in which k_s is the Nikuradse roughness length, usually related to some grain size percentile (e.g. $2.5d_{50}$, d_{90} , $3d_{90}$).

Subsequently, under nonuniform flow conditions in a similar bend, the net force in transverse direction varies over the water column (Van Bendegom, 1947). Near the bed the centrifugal force is considerably smaller than the pressure head, whilst near the water surface the centrifugal force outplays the pressure head (Van Bendegom, 1947; Engelund, 1974). This drives a secondary current from the outer to the inner bend via the bed – so, the local flow close to the bed deviates to the inner bend (Figure 2.1). In the inner bend the secondary flow resurfaces and starts flowing to the outer bend again, completing the vortex.

A commonly applied equation for the deviation angle of bed load transport due to secondary flow $\angle\delta$ was derived by Van Bendegom (1947), who considered four forces acting on a fluid element travelling under steady flow conditions in a channel bend: (1) streamwise water surface slope, (2) transverse water surface slope, (3) centrifugal force, and (4) Coriolis force.

$$\tan \delta = K \frac{h}{r} \quad (2.8)$$

where $\angle\delta$ is measured in the horizontal plane, positive toward the inner bend and K is a numerical factor that depends on the Chezy parameter. By and large, the Coriolis force is of negligible importance, for rivers are fairly slender. Van Bendegom (1947) identified K as a constant 10, assuming $C = 50 \text{ m}^{0.5}/\text{s}$. Other numerical constants were found by e.g. NEDECO (1959), Rozowskii (1961) and Engelund (1974) (see Table 2.1). In later studies (e.g. Kikkawa et al., 1976; Zimmerman, 1977; Odgaard, 1981; 1986), K is usually identified as a function of the Darcy-Weisbach friction factor f , given as (Silberman et al., 1963 in Kleinhans, 2005a):

$$f = \frac{8g}{C^2} \quad (2.9)$$

Odgaard (1981) found K to depend also on a normalised grain shape parameter ζ and the

particle densimetric Froude number $F_{*,cr}$ at the channel axis, given as

$$F_{*,cr} = \frac{\overline{u_{cr}}}{\sqrt{\frac{\rho_s - \rho}{\rho} g d_{50}}} \quad (2.10)$$

where $\overline{u_{cr}}$ is the critical mean flow velocity at the channel axis required for the given d_{50} to mobilise.

So, secondary flow transports sediment to the inner bend, contributing to the formation of a transverse slope. And because the drag exerted by secondary flow scales to the square grain diameter, finer grains are more effectively routed bend inward than coarser grains, neglecting interaction between differently sized grains.

Table 2.1: Expressions for K in eq. 2.8. A_r is a numerical constant, set at 8.5 (Kikkawa et al., 1976 & Ikeda et al., 1987).

Studies	K
Van Bendegom (1947)	10
NEDECO (1959)	8
Rozowskii (1961) in Zimmerman (1977)	<i>rough bed:</i> 11 – 11.5 <i>smooth bed:</i> 10 – 12
Engelund (1974)	7
Engelund (1975)	21
Engelund and Fredsoe (1982) in Bridge (1992)	10
Kikkawa et al. (1976) in Ikeda and Nishimura (1985)	$f \frac{-4.167u/u_* + 2.640/\kappa}{A_r}$
Zimmerman (1977)	$\frac{9.04 + 8\sqrt{f}}{3.83\sqrt{f} + 6.78f}$
Odgaard (1981)	$\frac{3\zeta}{2} \frac{\kappa\sqrt{8/f} + 1}{\kappa\sqrt{8/f} (2 + \kappa\sqrt{8/f})} F_{*,cr}^2$
Dietrich and Smith (1983)	$\frac{0.24}{f}$
Struiksma et al. (1985)	$-\frac{2}{\kappa^2} \left(1 - \frac{\sqrt{\theta}}{\kappa C} \right)$
Odgaard (1986)	$\frac{2\kappa\sqrt{8/f} + 1}{2\kappa^3\sqrt{8/f}}$
Ikeda et al. (1987)	$f \frac{r}{r_c} \frac{-4.167u/u_* + 2.640/\kappa}{\kappa A_r}$

2.2 Transverse bed slope effect

The second lateral force imposed on grains on a transverse slope is caused by gravity. Given a bed is inclined, a gravitational pull is exerted tangential to the bed on bed load particles, parallel to the slope direction (e.g. [Olesen, 1987](#); [Sekine and Parker, 1992](#)). This gravitational force is decomposed into a component parallel and perpendicular to the streamwise flow u_s . The former is usually of small-scale magnitude compared to the fluid drag component due to streamwise flow, and contributes to a negligibly small increase in bed load transport. The perpendicular component pulls sediment downward laterally, thereby causing a deflection of bed load transport on side slopes of channels and bars with respect to the streamwise fluid shear stress ([Sekine and Parker, 1992](#)). This effect is known as the transverse bed slope effect, and works in opposing direction to the secondary flow induced bed shear stress ([Van Bendegom, 1947](#); [Engelund, 1974](#)).

The transverse bed slope effect becomes larger with steeper transverse slopes, coarser grains and smaller bed shear stress, assumed similar flow conditions (e.g. [Schuurman and Kleinhans, 2013](#)). Additionally, a stronger transverse bed slope effect will result in gentler transverse slopes, which leads to fewer bars in the cross-section ([Schuurman et al., 2013](#)). So, the transverse bed slope effect influences braiding intensity.

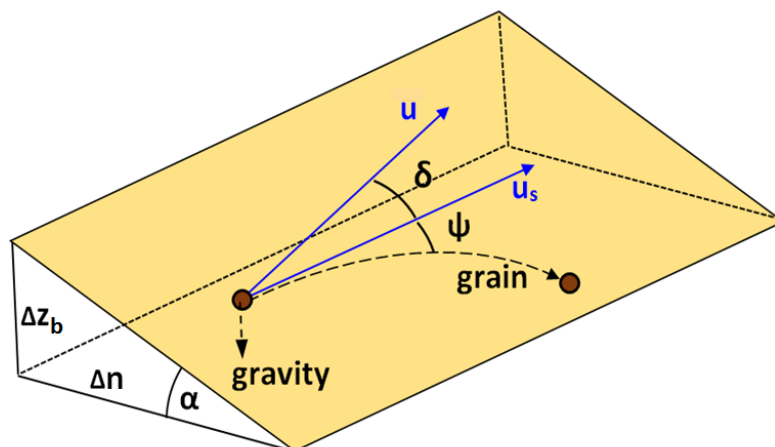


Figure 2.1: Deflection of sediment transport on a transversely inclined slope. On the one hand, gravity pulls down sediment perpendicular to the main flow u_s . On the other hand, secondary flow deflects the local flow velocity u and corresponding bed shear stress near the bed to the shallower, inward part of the bend, denoted with $\angle\delta$. The net deviation of these two effects is given as $\angle\psi$. (After [Schuurman and Kleinhans, 2013](#) and [Baar et al. \(in prep.\)](#))

2.3 Deviation angle of bed load transport

In the previous sections, the two dominant processes that influence transverse bed load transport were outlined. The transverse bed slope effect deviates bed load transport toward the pool (outer bend), whereas secondary flow counteracts this effect by routing sediment toward the point bar (inner bend). By combining these two mechanisms, the net deviation angle of bed load transport can be computed per local radius. Consequently, the equilibrium transverse bed slope, that is, the slope for which net deflection of sediment transport is zero, can be approximated. For the moment, uniformly sized sediment is considered.

In its simplest form, the net deviation $\angle\psi$ (Figure 2.1) is computed as the ratio between transverse and longitudinal bed load transport:

$$\tan \psi = \frac{q_n}{q_s} \quad (2.11)$$

where q is the bed load transport rate per unit width and the subscripts n and s are transverse and longitudinal coordinates, respectively.

The first physically derived equation for the transverse bed slope was given by [Van Bendegom \(1947\)](#), based on the aforementioned four forces that act on a grain to determine the direction of bed load transport on a transverse slope: (1) the fluid drag component due to mean flow, (2) the fluid drag component due to secondary flow, (3) the gravitational component parallel to the mean flow, and (4) the gravitational component perpendicular to the mean flow due to a transversely inclined slope. When the forces in transverse direction balance, net deflection of sediment transport is zero and hence, the transverse slope $\angle\alpha$ is in equilibrium. For this condition, [Van Bendegom \(1947\)](#) found

$$\sin \alpha = 10 \frac{h^2 S_n}{d_{50}} \frac{1}{r} \quad (2.12)$$

where S_n is the transverse water slope and d_{50} is the median grain size. The numerical constant includes the relative submerged density, the gravitational constant g and a constant bed friction coefficient ([Van Bendegom, 1947](#)).

The equation was adapted by [Koch and Flokstra \(1980\)](#) and [Struiksmma et al. \(1985\)](#) to take into account both the transverse and streamwise bed slope:

$$\tan \psi = \frac{\sin \delta - \beta \frac{\partial z_b}{\partial n}}{\cos \delta - \beta \frac{\partial z_b}{\partial s}} \quad (2.13)$$

in which β is a slope factor that depends on the dimensionless Shields parameter θ , and $\partial z_b / \partial n$ and $\partial z_b / \partial s$ are the transverse and longitudinal bed slope, respectively. The first term in the nominator represents the secondary flow, the second term the transverse bed slope effect.

The Shields parameter is of key importance for sediment mobility; it represents the ratio between bed shear stress and gravitational force that acts on the grains, given as

$$\theta = \frac{\tau}{(\rho_s - \rho)gd_{50}} \quad (2.14)$$

where ρ_s is the density of sand. In case of modelling sediment transport, the Chezy parameter related to skin friction (C') ought to be used to find the skin friction related bed shear stress τ' . This can in turn be used to find the skin friction related Shields parameter θ' .

The slope factor β in eq. 2.13 was (re)formulated in numerous studies. For a detailed summary of the formulations, the reader is referred to e.g. [Sekine and Parker \(1992\)](#) and [Odgaard \(1981\)](#). Most are based on narrow arrays of uniform grain sizes and flow conditions. [Engelund \(1974; 1975\)](#) and [Wiesemann et al. \(2006\)](#) found a numerical constant for β (Table 2.2) – β is only constant when the bed form regime is dunes, according to [Wiesemann et al.](#)

(2006). Other formulations found in literature show a dependence on the Shields parameter of the form

$$\beta = a_\beta \theta^{b_\beta} \quad (2.15)$$

where a_β is a calibration factor, either based purely on experimental data or based on comparison between model results and experimental data, and b_β is usually set at -0.5 (Table 2.2). The various slope factors vary up to an order of magnitude for a given θ . Excluding the numerical constants of Engelund (1974) and Wiesemann et al. (2006), all show a decrease in β with increasing θ , and therefore with finer grains and larger bed shear stress. This is reflected in steeper slopes, given the flow conditions ($\angle\delta$) are constant (Schuurman and Kleinhans, 2013; Baar et al., in prep.). Baar et al. (in prep.) is the only study in which the calibration factors a_β and b_β are not constant.

Resultant transverse slopes in natural rivers are found up to 0.3 (Figure 2.2). It is found that transverse slope decreases for wider channels. This is, because the narrow rivers had relatively much larger h -to- r ratios and therefore likely much stronger secondary currents.

The slope factor β and so, the deviation angle $\angle\psi$ depend on grain size. In case of non uniform sediment, this will lead to spatial separation based on grain size, which will be outlined in the following section.

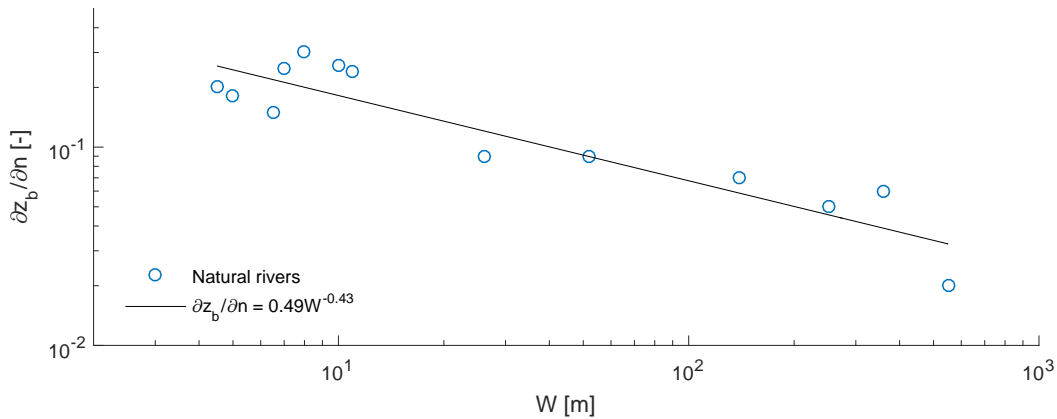


Figure 2.2: Transverse slope range of natural rivers. Narrow rivers generally had lower h -to- r ratios, leading to stronger secondary flow and steeper slopes. Data based on: Rozowskii (1961); Jackson (1975); Dietrich and Smith (1983); Thorne et al. (1985); Odgaard (1981; 1987); Julien and Anthony (2002); Clayton and Pitlick (2007).

Table 2.2: Expressions for β in eq. 2.13. Tested d_{50} are given when transverse bed experiments were conducted or experimental data of another study were used for model validation.

Studies	β	d_{50} tested [mm]	Flume type	Relevant notes
Engelund (1974)	$1/\tan\Phi$	0.3	Curved	–
Engelund (1981); Engelund and Fredsoe (1982)	$\frac{1}{1.6\sqrt{\theta}}$	–	–	–
Hasegawa (1981)	$\frac{1}{\sqrt{\mu_s\mu_d}} \left(\frac{\theta_{cr}}{\theta}\right)^{0.5}$	0.425	Straight	–
Ikeda (1982); Parker (1984); Parker and Andrews (1985)	$\frac{1 + \gamma\mu_d}{\lambda\mu_d} \left(\frac{\theta_{cr}}{\theta}\right)^{0.5}$	1.3 0.73, 1.2	Straight Curved	– Bend sorting field data
Struiksmā et al. (1985)	$\frac{1}{1.5\theta}$	0.3, 0.45, 0.6, 0.78	Curved	–
Ikeda et al. (1986; 1987)	$\frac{1 + \gamma\mu_d}{\lambda_{he}\mu_d} \left(\frac{\theta_{cr}}{\theta}\right)^{0.5}$	0.95	Curved	Bend sorting
Sekine and Parker (1992)	$0.75 \left(\frac{\theta_{cr}}{\theta}\right)^{0.25}$	0.425, 0.7, 0.83, 1.3	Straight & curved	–
Talmon et al. (1995)	$\left(9 \left(\frac{d_{50}}{h}\right)^{0.3} \sqrt{\theta}\right)^{-1}$	0.09, 0.16, 0.785	Straight	–
Sloff et al. (2001) in Sloff and Mosselman (2012)	$\left(A_{sh} \sqrt{\theta} \left(\frac{d_{50}}{h}\right)^{0.3} \left(\frac{d_{50,in}}{d_{50}}\right)^{D_{sh}}\right)^{-1}$	–	–	–
Parker et al. (2003)	$0.7 \left(\frac{\theta_{cr,0}}{\theta}\right)^{0.5}$	–	–	–
Ruther and Olsen (2005)	$0.6/\sqrt{\theta}$	0.6	Curved	–
Talmon and Wiesemann (2006)	$c \frac{1}{\mu_d} \left(\frac{\theta_0}{\theta}\right)^{0.5}$	0.09, 0.16, 0.78, 0.96	Straight	–
Wiesemann et al. (2006)	<i>ripples:</i> $\theta^{-0.5}$ <i>dunes:</i> 1.11	0.25, 0.96, 3	Straight	–
Baar et al. (in prep.)	<i>not yet determined</i>	0.17, 0.26, 0.37, 1, 2, 4	Rotating annular flume	Density varied

2.4 Sediment sorting in river bends

Sediment sorting in river bends can be categorised into two classes: bend sorting (lateral) and sorting by bed forms (vertical). First, bend sorting is explained starting from an ideal, infinite bend scenario and developed for natural meanders. Subsequently, vertical sorting at the lee side of bed forms is clarified.

2.4.1 Lateral: bend sorting

Firstly, a wide channel with constant curvature is considered with uniformly sized sediment. Flow in the bend focuses on the outer bend, leading to a higher flow velocity and bed shear stress in this section of the channel compared to the inner bend. Given the flow velocity is sufficiently large that the critical bed shear stress is exceeded, net erosion and deposition occur in the outer and inner bend respectively, until the lateral forces that act on the grains are in balance (Ikeda et al., 1987). At this stage, an equilibrium transverse bed profile is attained.

Secondly, a unimodal sediment mixture is taken into account in the same channel. Nonuniform sediment tends to sort out laterally in a river bend, where sediment is coarser in the outer bend and finer in the inner bend (e.g. Ikeda, 1989; Yen and Lee, 1995; Clayton and Pitlick, 2007); namely, coarser grains are pulled down more than finer grains, relative to the secondary flow induced bed shear stress, and assuming equal density. The according equilibrium transverse bed slope is therefore coupled to the lateral sorting (Ikeda et al., 1987). In natural meanders, the above described bend sorting is also observed, both in gravel bed rivers (e.g. Clayton and Pitlick, 2007) and sand bed rivers (e.g. Bridge and Jarvis, 1976 in Clayton and Pitlick, 2007; Dietrich and Smith, 1983).

Thirdly, the channel is assigned a sinuous shape with constant amplitude. Now, the flow pattern and hence the transverse bed profile and deviation of bed load transport are influenced by the upstream bend. Just before the bend curvature switches from clockwise to counterclockwise and vice versa (henceforth denoted as an inflection), highest flow velocities are found in the

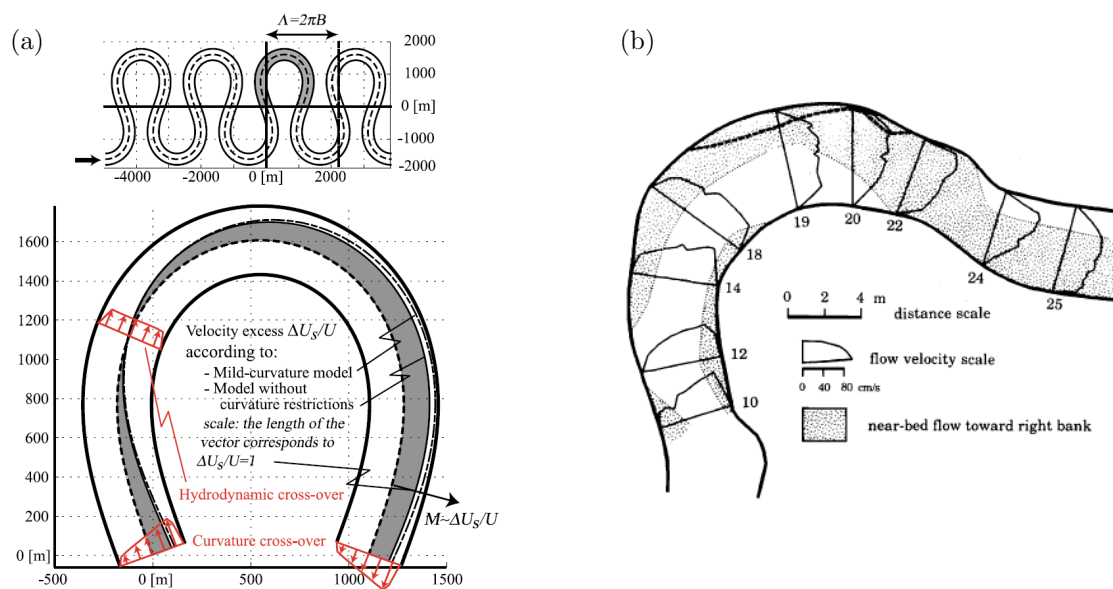


Figure 2.3: a) Vertically averaged longitudinal flow in an idealised meander bend. The grey section has largest flow velocities. Here, B is channel width and Λ is wave length (Blanckaert, 2011). b) Vertically averaged flow in a natural meander bend. The thick dotted line represents the bank position in 1976, the solid line in 1978 (Dietrich and Whiting, 1989).

outer bend. Moreover, the sediment is sorted laterally, similarly as described above, with a pool and point bar in the outer and inner bend, respectively. After the inflection however, the flow pattern has to adapt for flow to be able to make the curve. Consequently, also the transverse bed profile and associated lateral sorting will change in streamwise direction, advancing to a new equilibrium profile. As flow progresses, momentum is being redistributed until highest flow velocities are again in the outer bend (Figure 2.3a). The location where this occurs, is denoted as the hydrodynamic crossover. This implies that secondary flow also swaps direction along the way, as was seen in a natural meander of the Muddy Creek (Figure 2.3b) (Dietrich and Whiting, 1989).

So, bend sorting results in a fining upward trend from the outer to the inner bend. It is this trend that is preserved vertically in the point bar as the meander curvature expands due to channel migration.

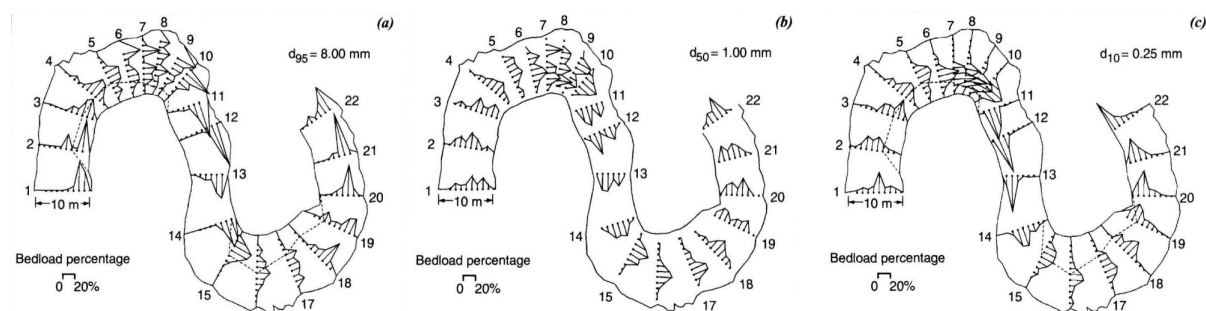


Figure 2.4: Bed load transport vectors for three mass percentile fractions of the bulk sediment over the channel width for 22 cross sections. a) $d_{95} = 8 \text{ mm}$; b) $d_{50} = 1.0 \text{ mm}$; c) $d_{10} = 0.25 \text{ mm}$. (Julien and Anthony, 2002)

In a field campaign in the Fall River, Colorado (US), both the reversal of bend sorting along a river bend and the hydrodynamic crossover were identified (Figure 2.4) (Julien and Anthony, 2002). Sediment samples at 22 transects showed that d_{95} is routed strongly to the outer bend and d_{10} to the point bar; just before the inflection, lateral sorting is best developed. At the inflection, the d_{10} , d_{50} and d_{95} are transported quasi-parallel. The adaption lengths of main flow and bed to disturbances such as a change in channel curvature were defined using a linearised model by Struiksmma et al. (1985).

Additionally, the adaptation of lateral sorting to a new bend is recognisable on a point bar

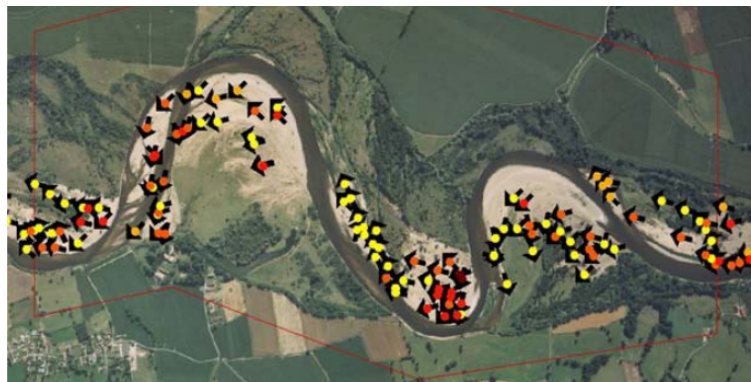


Figure 2.5: Sorting on and along point bars of the Allier. Flow is from right to left. Colours indicate grain size, ranging from sand (yellow) to cobbles/pebbles (red/brown); arrows indicate local flow direction. (Van den Bosch, 2003)

(Julien and Anthony, 2002). Just after an inflection there is still relatively coarse sediment present next to a point bar. In streamwise direction, the inner bend becomes finer due to the adjusting lateral sorting. Therefore, the upstream part of a point bar is slightly coarser than its downstream part, which also seems to be the case for the Allier (FR), a mixed sand-gravel bed river (Figures 2.4 & 2.5).

In mixed sand-gravel bed rivers, a second effect may enhance coarsening of the upstream part of a point bar: widening of the river at an inflection causes flow to decelerate. Because the coarser fraction is significantly less mobile than the finer fraction, gravel may be deposited at the upstream end of a point bar. This was observed in the Allier as well (Kleinhans, 2002).

In three experimental studies (Ikeda et al., 1987; Yen and Lee, 1995; Yen and Lin, 1997), attempts were made to create and study bend sorting under a very restricted range of flow conditions and size gradations. The main findings of these studies are summarised below.

Ikeda et al. (1987) determined the lateral distribution of grain size in a uniformly curved flume ($r_c = 1.2$ m, $W = 0.3$ m, angle = 270°) by taking sediment samples at morphodynamic equilibrium (Figure 2.6a). They used a poorly sorted, coarsely-skewed sediment mixture with an initial median grain size $d_{50,in} = 0.95$ mm (i.e., before sorting had occurred). Ikeda et al. (1987) related normalised grain size $d_{50}/d_{50,in}$ to normalised lateral location r/r_c , which can be approximated by

$$\frac{d_{50}}{d_{50,in}} = a \left(\frac{r}{r_c} \right)^b \quad (2.16)$$

where a and b are empirical coefficients. Ikeda et al. (1987) found $a = 0.95$ and $b = 10.2$. In the experiment, roughly uniform flow conditions were applied that disfavoured bed form formation.

Yen and Lee (1995) tested the effect of different hydrographs on bend sorting and bed slope development in a uniformly curved flume ($r_c = 4$ m, $W = 1$ m, angle = 180°) (Figure 2.7). They used a sediment mixture with $d_{50,in} = 1$ mm with unclear skewness and modality under roughly uniform flow conditions. The transverse bed slope was largest and bend sorting was most apparent near 90° , and became more distinct with larger peak flow (Figure 2.6). Lateral

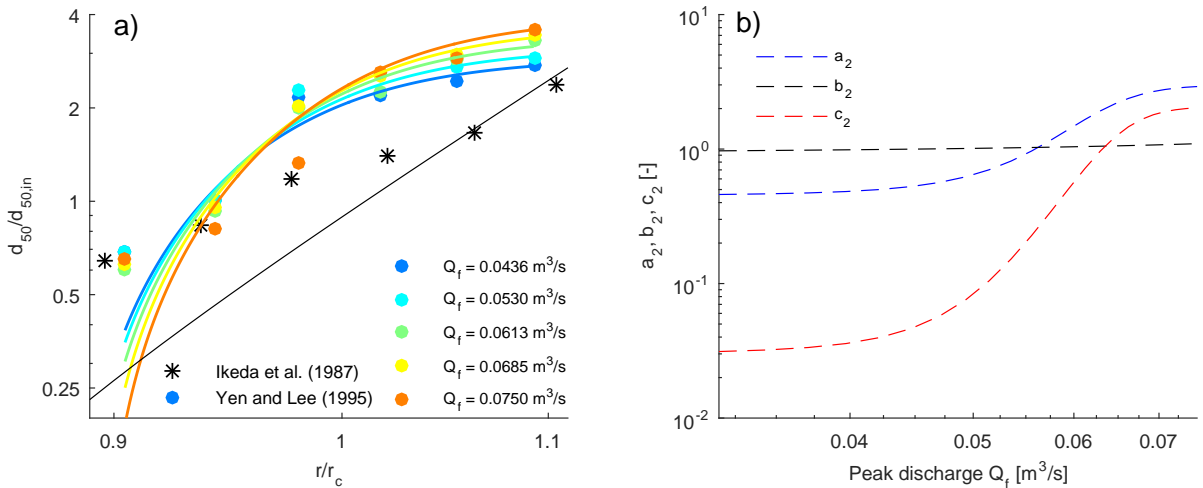


Figure 2.6: a) Lateral sorting in two experimental studies (Ikeda et al., 1987; Yen and Lee, 1995). Median grain size, normalised to the median grain size of the initial mixture, plotted against the normalised lateral location in the bend. Markers represent the samples, the regressions the best approximation (Yen and Lee, 1995) and prediction (Ikeda et al., 1987). b) Best fit of the empirical coefficients in eq. 2.17 as function of peak discharge. (Yen and Lee, 1995)

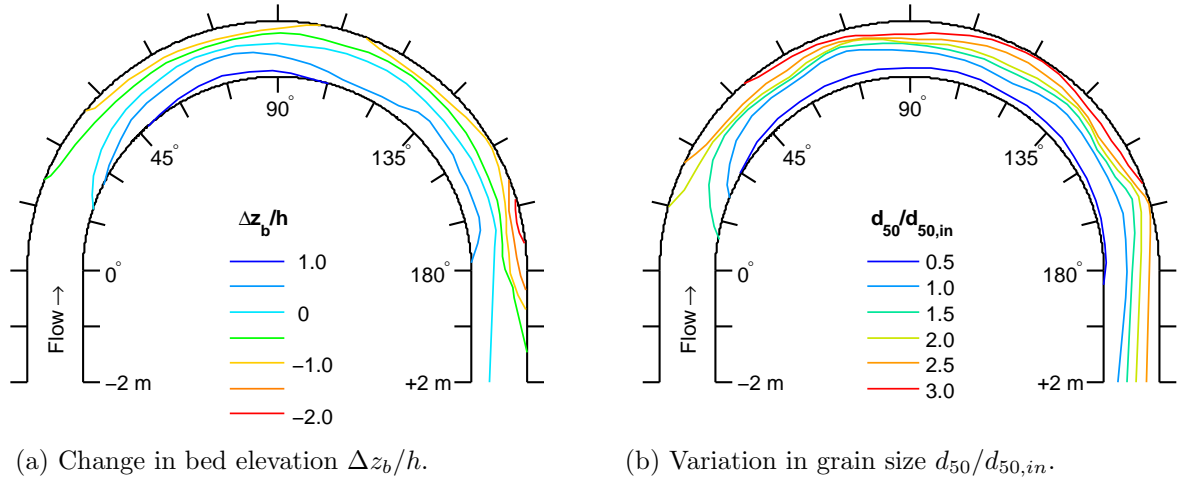


Figure 2.7: Transverse bed development and bend sorting in a 180° degree flume bend for the highest peak flow condition ($Q_f = 0.075 \text{ m}^3/\text{s}$ in Figure 2.6), in which $\Delta z_b/h$ is the bed deformation relative to the initial water depth. $\Delta z_b/h$ is negative if erosion had taken place, positive if deposition had occurred. The 11.5 m long straight reaches before and after the bend are left out of the figures. (Yen and Lee, 1995)

variation in d_{50} was approximated by

$$\frac{d_{50}}{d_{50,in}} = a_2 \tanh \left[10 \left(\frac{r}{r_c} - b_2 \right) \right] + c_2 \quad (2.17)$$

in which a_2 , b_2 and c_2 are coefficients that depend on the peak flow in the hydrograph (Figure 2.6b) (Yen and Lee, 1995). Once flow exited the bend, lateral sorting and the transverse bed slope decayed. Flow conditions were chosen such that bed forms would not form.

The findings of Yen and Lee (1995) were approached reasonably well with a 3D numerical model with the Van Rijn bed load transport equation for uniform sediments (Fischer-Antze et al., 2009; Van Rijn, 1984a). Yet, the height of the inner bend's bed was over-estimated and sorting was predicted inadequately. This improved considerably by including hiding and exposure effects in the sediment transport equations. This led to the conclusion that these effects are of significant importance in the transverse bed slope development and bend sorting (Fischer-Antze et al., 2009).

Yen and Lin (1997) studied the effect of initial size gradation σ_{in} on the lateral distribution of grain size in the same flume as Yen and Lee (1995). $d_{50,in}$ was kept constant at 1 mm. Yen and Lin (1997) found that the outer bend becomes coarser and the inner bend finer with larger σ_{in} once an equilibrium transverse bed had formed. This is likely for there is more to sort laterally. Additionally, the standard deviation increased in general from the inner to the outer bend.

All grain sizes experience higher mobility due to lateral sorting (Clayton and Pitlick, 2007): the hiding effect of fine grains amidst of larger ones diminishes in the inner bend as coarser grains are diverted toward the outer bend, whereas coarser grains are exposed to relatively large bed shear stress in the outer bend. Additionally, the relative coarsening of the pool's bed enhances the local transverse bed slope effect, resulting in a shallower equilibrium pool depth (Ikeda et al., 1987; Schuurman and Kleinhans, 2013).

Discharge relative to bankfull discharge influences lateral sorting (Clayton and Pitlick, 2007; Blanckaert, 2011). As discharge increases toward bankfull conditions, coarse and fine grains are routed more effectively to the outer and inner bend, respectively. For discharges that exceed bankfull conditions, the focus of the coarse fraction relocates more toward the middle part of

the bend. It is hypothesised that this shift is caused by relative straightening of the channel with large discharge, which leads to slight unbending of bed load transport ([Bridge and Jarvis, 1976](#) in [Clayton and Pitlick, 2007](#)).

[Clayton and Pitlick \(2007\)](#) have shown using field data that mobility in the inner bend is restricted to the finer grain size fraction due to relatively small shear stress, whilst in the outer bend all size fractions are mobile. The latter is the case for discharges that exceed two-thirds bankfull discharge ([Clayton and Pitlick, 2007](#), which coincides with the mobility threshold for armour-layer particles ([Mueller et al., 2005](#))). For lower discharges and especially wide sediment mixtures, an armour layer may form. In mixed sand-gravel bed rivers such as the Allier (FR), the gravel fraction in the inner and outer bend can both be considerable ([Kleinhans, 2002](#)), which suggest poor lateral sorting for such river types.

2.4.2 Vertical: sorting by bed forms

Sediment is arranged in bed forms when the critical bed shear stress is exceeded, where the type of bed form depends on the applied Shields stress and the Bonnefille number D_* , which is dimensionless grain size (Van Rijn, 1984a; Van den Berg and Van Gelder, 1993; Kleinhans, 2005a):

$$D_* = d_{50} \sqrt[3]{\frac{(\rho_s - \rho)g}{\rho\nu^2}} \quad (2.18)$$

in which ν is the kinematic viscosity of water. The Shields curve describes the threshold of motion and like all boundaries between bed form types should be considered as transitional. Furthermore, the Shields curve only applies to sediment mixtures with relatively narrow ranges of grain sizes, so that hiding and exposure effects are minimal (Kleinhans and Van Rijn, 2002). Otherwise, fine particles are protected by coarser ones and therefore require large shear stresses to be mobilised. Coarser grains on the other hand would stick out relatively far in the water column compared to immediate surrounding particles, and therefore have relatively small critical bed shear stresses.

Vertical sorting occurs at the lee side of dunes as laminae are deposited, which is described as a three-phase-process (Kleinhans, 2005b). First, sediment is deposited on the lee slope by means of grain fall that is initiated at the dune's brinkpoint. Grain fall happens size selectively, with coarser grains being deposited higher upslope than finer grains due to their larger mass and hence, larger settling velocity. Most size fractions contribute to the formation of a wedge on

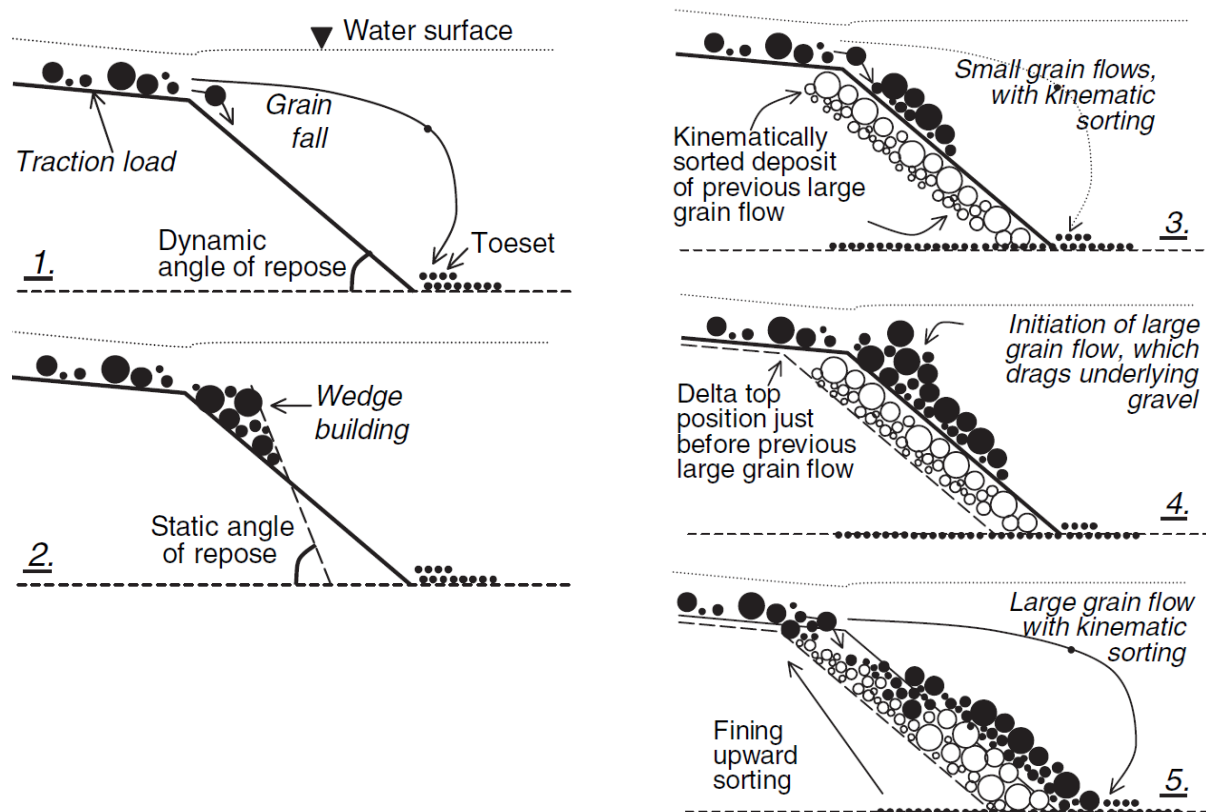


Figure 2.8: Three-phase-process of sediment deposition and sorting on lee slopes of experimental deltas, analogous to dunes, that leads to fining upward: 1,2: development of wedge and toe set, 3: small grainflows rework coarse grains upward, 4,5: coarse grains are dragged downslope by larger grainflows. (Kleinhans, 2005b)

the upper lee slope (Figure 2.8.1-2). The finest fraction may settle slow enough to be deposited in the trough, thereby forming a toe and bottomset. So, at first the deposit by grain fall tends to lead to a coarsening upward trend. Second, the newly deposited grains on the upper lee slope are transported downslope as grainflows once the static angle of repose is overcome. Kinematic sieving in small grainflows gives rise to coarse grains being reworked to the top of the flows (Figure 2.8.3). Third, large grainflows drag the top, coarse fraction of the previous grainflow downslope, resulting in a net fining upward trend in the laminae of dunes (Figure 2.8.4-5). Grainflows are deposited at the dynamic angle of repose, which is smaller than the static angle of repose, thus making it possible for the three-stage-process to start anew.

Vertical sorting by grainflows has been reviewed qualitatively by [Kleinmans \(2004\)](#) to depend on sediment mixture characteristics and flow velocity relative to the settling velocities of all size fractions. Intuitively, a sediment mixture with a larger standard deviation leads to more pronounced sorting for there is more to sort ([Kleinmans, 2004](#)). Yet, the shape of the grain size distribution (unimodal, bimodal, degree of skewness) influences the vertical sorting by affecting the angle of repose of larger grains on smaller ones and the kinematic sorting efficiency. Flow velocity relative to the settling velocities of all grain sizes determines the volume of grainflows by affecting the extent and thus, volume of the upslope wedge. A larger flow velocity contributes to a longer wedge, since particles can be deposited further from the brinkpoint. Given the static and dynamic angles of repose are unaltered, this leads to a more voluminous wedge. When the wedge fails, a thicker grainflow occurs which negatively affects kinematic sorting efficiency ([Kleinmans, 2004](#)).

2.5 Effect of bed forms on the slope factor β

Slope factors are found to be larger in flume experiments than in natural rivers (Talmon et al., 1995). This is likely caused by bed forms, which are much higher in flumes than in natural rivers, compared to the water depth. This scale issue can be described as (Van Rijn, 1984b):

$$\frac{\Delta}{h} = 0.11 \left(\frac{d_{50}}{h} \right)^{0.3} (1 - e^{-0.5T})(25 - T) \quad (2.19)$$

where Δ is bed form height and T is the transport stage parameter, given as

$$T = \frac{(u_*)^2 - (u_{*,cr})^2}{(u_{*,cr})^2} \quad (2.20)$$

in which $u_{*,cr}$ is the critical bed shear velocity. Disregarding anti-dunes, bed forms are assumed to exist only for $T[0 - 25]$ (Van Rijn, 1984b). Incorporation of the nonlinear dependence of Δ/h on the d_{50}/h ratio in the slope factor has resulted in a better approximation of transverse bed slopes (Talmon et al., 1995) (see Table 2.2).

Furthermore, the type of bed form that covers the bed seems to affect the slope factor as well (Wiesemann et al., 2006; Baar et al., in prep.); Wiesemann et al. (2006) recognised a drop in β when the bed form type shifted from three dimensional ripples to dunes, meaning the transverse slope became steeper. In contrast, Baar et al. (in prep.) found a decrease in transverse bed slope for the same transition, which suggests that β had increased. However, this increase was also observed for coarser uniform sediments with dunes prevailing under all tested conditions. Therefore, it is still inconclusive whether it is solely bed forms that cause the sudden increase in β (Baar et al., in prep.).

2.6 Flume types used in previous research

In this section, the use and (dis)advantages of three types of flumes are described with which transverse bed slope development and bend sorting experiments were conducted. First, straight flumes are discussed, followed by curved flumes and rotating annular flumes.

2.6.1 Straight flumes

Straight flumes differ from their curved counterparts in that secondary flow is often neglected (Talmon et al., 1995). This doubtlessly explains why sorting in straight flumes has practically not been examined, since a force that opposes the transverse bed slope effect is lacking. Given the longitudinal slope is negligible, eq. 2.13 reduces to

$$\tan \psi = -\beta \frac{\partial z_b}{\partial n} \quad (2.21)$$

Generally, straight flume experiments start with an initially inclined, either sinuous or straight transverse slope (Figure 2.9) that is subjected to given flow conditions. In time, the transverse slope decreases as bed load transport is deflected downwards, where the bed levelling time scale together with q_s is a measure for β (Talmon et al., 1995).

Advantageous of straight flumes is the isolation of the transverse bed slope effect from the bed load deviation by secondary currents (Talmon et al., 1995). However, this is also a drawback: the equilibrium transverse slope and lateral sorting cannot be determined.

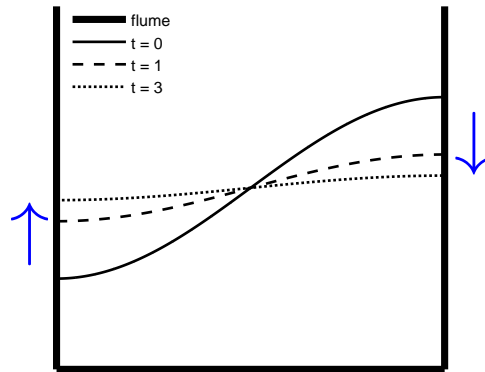


Figure 2.9: Schematic cross-section of a bed levelling experiment in a straight flume, starting with an initial sinuous transverse slope. Flow is either in or out of the paper. As time passes, the bed levels, where the bed levelling time scale together with streamwise sediment transport is a measure for the slope parameter. Timestep t is the time required for a e^{-1} reduction of the amplitude of the sinuous bed.

2.6.2 Curved flumes

Several studies in this field of expertise used curved flumes to study the development of transverse bed slopes (e.g. Engelund, 1974; Struiksmas et al., 1985; Ikeda et al., 1987) and bend sorting (Ikeda et al., 1987; Yen and Lee, 1995; Yen and Lin, 1997). For a thorough review on tested radii, θ and findings, the reader is referred to e.g. Odgaard (1981) and Wiesemann et al. (2006).

Curved and straight flumes are unclosed systems, which means that sediment must be introduced upstream of the test location in the flume to mitigate unwanted loss of sediment at the test location. This can be realised by (1) sediment feeding and (2) sediment recirculation, both of which are hypothesised to influence dune and vertical sorting dynamics (Kleinmans, 2005c). For example, coarse lag layers can form in dune troughs when sediment is recirculated.

Both secondary flow and the transverse bed slope effect are simulated in a curved flume, which makes it possible to determine the equilibrium transverse slope and lateral sorting. Nonetheless, the effect of the transverse bed slope cannot be isolated from the sediment mobility. Hence, the range of experiments is restricted.

2.6.3 Rotating annular flumes

A third type of flumes that can be used is rotating annular flumes (also known as carousel flumes) (Figure 3.1) (used by Baar et al., in prep.). Flow is initiated by a rotating lid. Counter-rotation of the flume itself with respect to the lid generates a centrifugal force on the lower part of the water column, thereby weakening secondary flow intensity (Booij and Uijttewaal, 1999). Essentially, the flume can be considered an infinitely long, uniformly curved bend.

Consequently, the transverse bed slope effect and the effect of secondary flow can be isolated (e.g. Booij, 1994), making carousels more advantageous than straight and curved flumes for studying spatial sorting. Additionally, rotating annular flumes are closed systems, meaning they lack effects of in and outflow. However, a complex 3D flow pattern arises in the annular flume, especially when counter-rotation of the flume is applied (Booij, 1994).

The deviation of bed shear stress by secondary flow $\angle\delta$ was approximated for an annular flume by determining the u_n/u_s ratio for varying rotation speeds of lid and flume (Baar et al., in prep.):

$$\delta = \arctan(u_n/u_s) \quad (2.22)$$

$$u_n = \frac{A_1 \bar{h} W}{r_c (A_2 f_g W + A_2 f_g \bar{h} + A_3 f W)} \cdot (A_4 \omega_{btm} r_c + A_5 \omega_{lid} r_c) \quad (2.23)$$

$$u_s = \frac{|\omega_{lid} r_c - 0.5 \omega_{btm} r_c|}{2A_s} \quad (2.24)$$

where ω_{lid} and ω_{btm} are the rotation speeds of the lid and flume (in rad/s), A_{1-5} and A_s are calibration factors and f_g is the Darcy-Weisbach friction factor related to the glass sidewalls of the carousel. Counter-rotation of the flume is denoted as a negative ω_{btm} . Baar et al. (in prep.) found for their carousel: $A_1 = 1/40$, $A_2 = 1$, $A_3 = 1$, $A_4 = 2.5$, $A_5 = 1$ and $A_s = 0.65$. Flume dimensions are given in Figure 3.1.

2.7 Gaps in knowledge

Bend sorting theory provides an explanation for why the outer bend is coarser than the inner bend (Ikeda et al., 1987), but it is unclear how the degree of lateral sorting responds to changes in boundary conditions. Previous experiments are very limited and were conducted in curved flumes, which disallow the isolation of the transverse bed slope effect and sediment mobility. Recent advances in a rotating annular flume showed that this flume type is more promising.

In natural meanders, sediment is sorted laterally according to the bend sorting theory and vertically by bed forms. Until present, the interplay of these two sorting mechanisms has not been studied experimentally – previous sorting experiments applied flow conditions that disfavoured bed form formation. This leads to the question whether bed forms (1) are superimposed on lateral sorting, i.e. just sort the sediment that is available at a certain radius as a consequence of lateral sorting or (2) also modify lateral sorting.

2.8 Hypotheses

Based on the theoretical background, multiple hypotheses are formulated to the above presented knowledge gaps, that will be tested experimentally in a rotating annular flume.

Grains in a non-uniform mixture tend to sort out laterally in river bends based on grain size due to differences in deviation angles $\angle\psi$ (Ikeda et al., 1987). One of the key factors influencing lateral sorting is the transverse slope. On such a slope, grains are dragged inward by secondary flow, scaling to the square of the grain size, and pulled down by gravity, which scales to grain size to the power three. As secondary flow intensity increases, a steeper transverse slope will form, and the aforementioned nonlinearity that separates grain size laterally is hypothesised to increase. So, the first hypotheses are:

1. Lateral sorting develops on a transversely inclined bed in a river bend.
2. Lateral sorting becomes more pronounced with steeper transverse slopes.

Bed forms sort grains vertically in a fining upward trend that becomes more distinct with lower flow velocity (Kleinhans, 2005b). Analogously, it is believed a lower flow velocity will contribute to more pronounced lateral sorting due to less turbulence. Furthermore, bed forms likely sort the sediment vertically that is made available by lateral sorting: a relatively coarse fining upward trend in the outer bend and fine fining upward trend in the inner bend. Finally, field research in the Gelsa River (DK) showed that the orientation of dunes in the inner bend may lead to the generation of transverse currents (Kisling-Moller, 1993). The *skewed* bed forms act as obstacles of flow and generate a corkscrew flow. This may influence lateral sorting strongly on the local scale. So, the final hypotheses are:

3. Lateral sorting becomes more distinct with lower sediment mobility.
4. Bed forms sort sediment vertically that is made available by lateral sorting.
5. Bed forms cause longitudinal variability in lateral sorting on the bed form length scale.

3 Materials & methods

Until present, it is unclear how the degree of lateral sorting depends on changes in boundary conditions. Therefore, an experimental approach was chosen to make a first assessment, namely of the effect of the transverse slope and sediment mobility on lateral sorting. To this end, a rotating annular flume was used, identical to the one used by Baar et al. (in prep.). With such a flume, morphodynamic equilibrium conditions could be attained, because the flume is essentially an infinitely long, uniformly curved bend, and the effect of the tested parameters could be isolated.

In this chapter, the methods are described, starting with the experimental setup, including the sediment mixture used in this study. Then, the experimental conditions are outlined, and finally, the data acquisition is discussed.

3.1 Experimental setup

Experiments were conducted using the Cees Kranenburg 'donut-shaped' carousel flume in the fluid mechanics lab at TU Delft (Figure 3.1). The flume's bend radius at the channel axis is $r_c = 1.85$ m, its width $W = 0.30$ m and its height 0.47 m. The flume is topped with a rotatable lid that is in direct contact with the water, and can initiate a current by dragging water along as it spins. For this study, the lid was set at 0.36 m above the steel floor of the flume.

A small, near-unimodal sediment mixture was used with median grain size $d_{50,in} = 0.75$ mm, and first standard deviations of $d_{16,in} = 0.52$ mm and $d_{84,in} = 1.43$ mm (Figure 3.3). This mixture was hypothesised to be close to equimobility due to the small nature of the sediment distribution. Consequently, hiding and exposure effects that may affect the transverse slope were assumed negligible.

A sand body of 0.15 m thick was planted in the flume, so $\bar{h} = 0.21$ m. Before each experiment, the sediment was mixed to remove potential effects of sorting of former experiments. Ideally, all size fractions were evenly distributed over the sand body. Subsequently, the bed was smoothed to acquire an initial flat bed from which a transverse bed slope, bed forms and spatial sorting developed. Experiments were stopped once morphodynamic equilibrium was reached. Such equilibrium is met when bed form height and length, and lateral and vertical sorting are

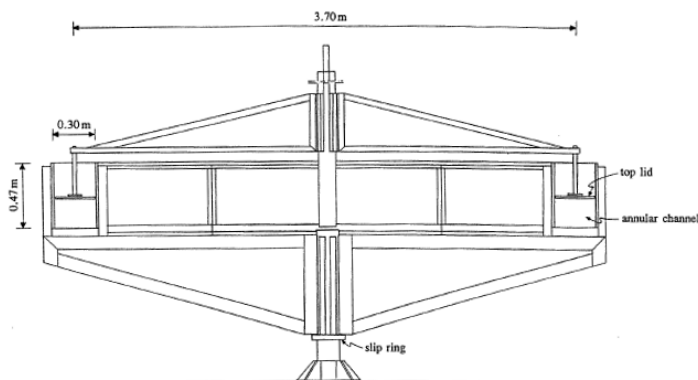


Figure 3.1: Cees Kranenburg carousel flume with $W = 0.3$ m, $r_c = 1.85$ m and $\bar{h} = 0.21$ m. (Booij, 1994)

approximately stable over time. Experiments were terminated when fluctuation of the number of dunes in the flume persisted. Generally, the experiments run for two to three days.

Secondary flow intensity was reduced by counter rotating the flume itself (see section 2.6.3) (Booij and Uijtewaal, 1999), leading to a smaller $\angle\delta$. Consequently, larger bend radii could be simulated. All variables that influence the spatial sorting could be isolated for a given sediment mixture by varying the rotation rates of the top lid and the flume itself.

3.2 Experimental conditions

A total of 34 experiments were conducted with varying secondary flow intensity and sediment mobility, where the latter was varied between $\theta/\theta_{cr} = 1.1$ and 6. It was hypothesised that the bed form regime under this sediment mobility range was dunes (Van den Berg and Van Gelder, 1993), and that lower mobility would lead to immobility of the coarse fraction and to a bed form shift to ripples. Based on eq. 2.19, a maximum dune height of 6.9 cm \pm a factor 2 was expected.

Dune height positively influences the thickness of the active layer, which affects the rate of lateral sorting response compared to the rate of morphological response. When lateral sorting develops relatively quickly, the transverse bed slope development is hypothesised to be hampered, especially in case of wide mixtures. On the other hand, bed forms are hypothesised to have an impact on the transverse slope (e.g. Wiesemann et al., 2006; Baar et al., in prep.). So, relatively high dunes with a maximum dune height up to $\Delta = 10$ cm were preferred. This corresponds to $\Delta/\bar{h} \leq 0.48$.

Experiments were selected for analysis of spatial sorting when the morphology resembled natural rivers best, namely transverse slopes between 0 and 0.25. These experiments were categorised as *sorting experiments*, and the remaining experiments as *morphology experiments*. Five experiments were not analysed due to (1) one or more dune troughs touching the hydraulically smooth steel floor of the flume, (2) evolution into an immobile state, (3) a malfunctioning of the bed level recording mechanism, and (4) an early termination for international visitors.

A third type of experiment, conducted only once, involved monitoring the development of the transverse bed during the first hour. To this end, experimental settings with relatively small streamwise flow and strong secondary currents were used, with the purpose that the bed advanced slowly but surely to a steep transverse bed slope. Because the water was usually turbid during the early stage of the experiments due to prior mixing of the bed, it is assumed that the transverse bed slope development occurred in a like manner in all experiments, though at different rates.

3.3 Data acquisition and processing

Bed elevation was scanned during and after for all experiments. This was done using an echo sounder (10 Hz sampling rate; footprint ~ 2 cm) attached to the lid – the effect of the echo sounder on flow conditions was assumed negligible. The echo sounder measured bed elevation profiles for 10 radii with 2.3 cm interval, disregarding the inner and outer 4.65 cm.

The echo sounder was removed from the lid during experiments with large rotation velocities. Therefore, bed elevation of such experiments was scanned afterwards only. Unfortunately, a malfunctioning of the echo sounder had occurred during experiment 29. The required repair may have altered the measured radii slightly since.

A digital elevation model (DEM) was created out of a point cloud of bed elevation measurements, obtained by the final scan after an experiment had ended. Increments of the point cloud were 2.3 and ~ 1 cm in n and s directions, respectively. Subsequently, the transverse bed slope was estimated as a linear regression through the median bed elevation per scanned radius.

Only sorting experiments were studied in further detail. This involved taking photographs of the dry bed, and taking sediment samples at distinct places dotted over the dunes, explained below. Photographs were taken of the end result with a Canon Powershot a640 (10 MP) of interesting bed form configurations and sorting effects, usually taken as side-views or panoramas. Drainage of the flume, needed to analyse the experiment, usually disrupted at least one dune.

Sediment sampling

Sediment samples were taken at five radii, and at three locations over the dune to capture the degree of spatial sorting (Figure 3.2). These were taken as bulk samples at the lee side of dunes and as surface samples at the dune top and in the dune trough.

Bulk samples were taken over the entire vertical deposit of a bed form, and were used to get insight in the actual transport per radius. The lee side was removed up to the brink point before a sample over the vertical deposit was taken (see Figure 3.2). Otherwise, the fraction of sediment in the bottom and toe set would be overblown compared to the top and foreset.

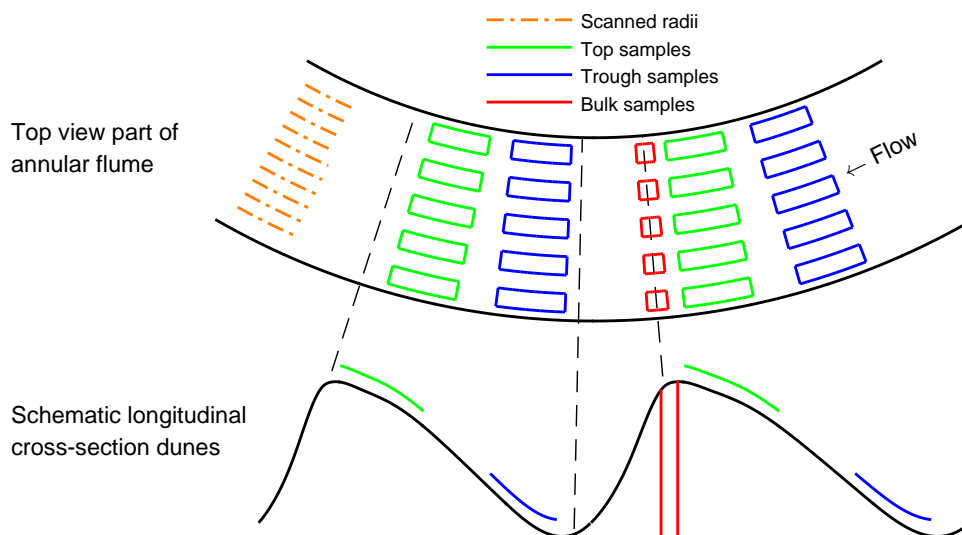


Figure 3.2: Schematic representation of sampling and scanned bed elevation radii. Two dunes were required for a single surface sample per radius. Bulk samples were taken over the entire vertical deposit after removal of the lee side up to the dune's brinkpoint. Samples for determining vertical sorting (in experiments 19 and 34) were taken at a similar location as bulk samples with vertical intervals of about 1 cm.

Surface samples were taken as strips of about 0.2 cm thick, 4 cm wide and 20 cm long. To acquire sufficient sediment for a sieve sample, two dunes were used to create one sample per radius, both for the dune top and trough. Furthermore, surface samples were done in twofold to examine internal variability. To do so, the standard deviation of two like samples was computed, after which the two were averaged. A limiting factor to the quantity of surface samples taken was the number of intact, fully grown dunes after drainage.

In addition to the above described samples, two sets of samples were taken to determine the vertical sorting at the outer and inner bend, namely in an experiment with a near-horizontal slope (n° 19) and with a steep slope (n° 34). Over the vertical deposit, samples were taken of roughly 1 cm thick. Moreover, surface samples were taken at sections of the flume were ripples covered at least half of the flume's width. The latter were restricted to two experiments with $\partial z_b / \partial n$ close to 0, namely experiments 19 and 26.

For each sample the grain size distribution was determined by means of mechanical sieving, as well as the median (d_{50}), and first (d_{16} , d_{84}) and second (d_{05} , d_{95}) standard deviations, where the subscripts mark the percentage of particles that are finer. These were used to estimate the inclusive standard deviation (Folk, 1968):

$$\sigma = \frac{d_{84} - d_{16}}{4} + \frac{d_{95} - d_{05}}{6.6} \quad (3.1)$$

and skewness:

$$Sk = \frac{d_{16} + d_{84} - 2d_{50}}{2(d_{84} - d_{16})} + \frac{d_{05} + d_{95} - 2d_{50}}{2(d_{95} - d_{05})} \quad (3.2)$$

where the standard deviation and skewness of the initial sediment mixture are $\sigma_{in} = 0.47$ mm and $Sk_{in} = 0.48$.

The sieved experiments were categorised into three $\partial z_b / \partial n$ classes: near-horizontal slopes (≤ 0.07), mild slopes ($0.07 - 0.15$) and steep slopes (≥ 0.15), and three θ / θ_{cr} classes: low (≤ 1.5), medium ($1.5 - 2.5$) and high (≥ 2.5). The effect of θ / θ_{cr} was determined by considering the steep slopes class only; this was done to mitigate the effect of the transverse bed slope, yet

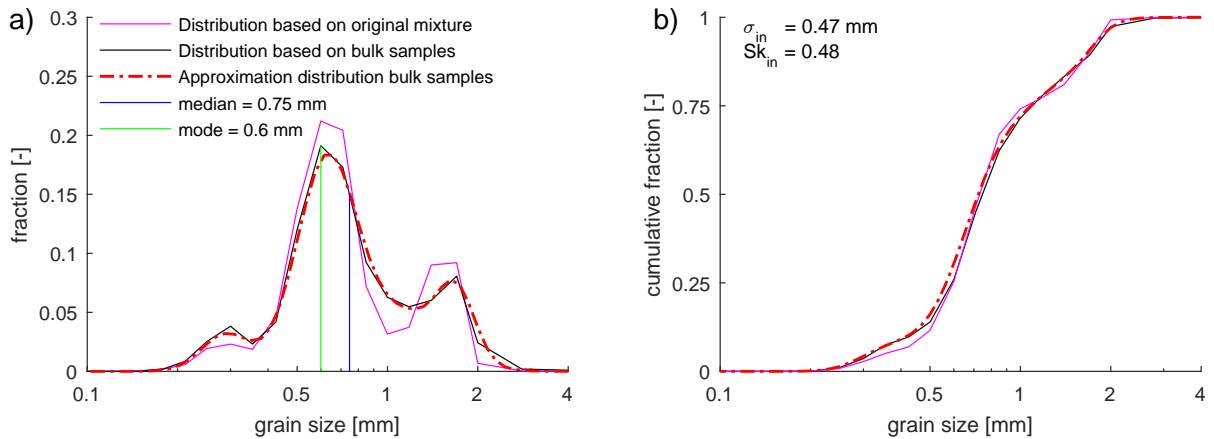


Figure 3.3: Grain size distribution of the sediment mixture used in this study as a) fraction and b) cumulative fraction. The distribution of the original mixture is the mean of two samples taken of the original mixture (i.e. before planted in the flume). These two samples were very dissimilar (not depicted here). The distribution based on all bulk samples is approximated by combination of four log normal distributions. The median, mode, standard deviation and skewness are all based on the bulk sample distribution, which was taken as initial mixture distribution in this study.

have sufficient lateral variation of d_{50} .

The initial sediment mixture distribution was approached by averaging the bulk samples of all experiments, excluding surface samples (Figure 3.3). The latter are about equal in size, yet volumetrically speaking, more sediment is transported in the inner bend than in the outer bend when the equilibrium transverse slope is nonzero. Since this process is not captured in surface samples, using these will relatively coarsen the mean sediment distribution. Two samples that were taken of the original sediment, i.e. before being planted in the flume, were too dissimilar to be used to determine the initial distribution accurately.

4 Results

In this chapter the results of this study are presented. First, preliminary results are given below. Next, the development of the experiments toward morphodynamic equilibrium is described qualitatively in terms of morphology and spatial sorting. Then, the effect of transverse bed slope and sediment mobility on spatial sorting is explained. Finally, the dimensions of and vertical sorting by bed forms are presented.

In total, 13 sorting experiments were conducted and 340 samples were taken. The flow- and morphology-related parameters are given in Table 4.1. Although the transverse slope of experiment 21 was too large, it was assigned to the sorting experiments as well, because a better alternative with high mobility was lacking. Over all experiments, it is found that steeper slopes formed with stronger secondary currents, i.e. smaller $\omega_{btm}/\omega_{lid}$, and larger θ (Figure 4.1).

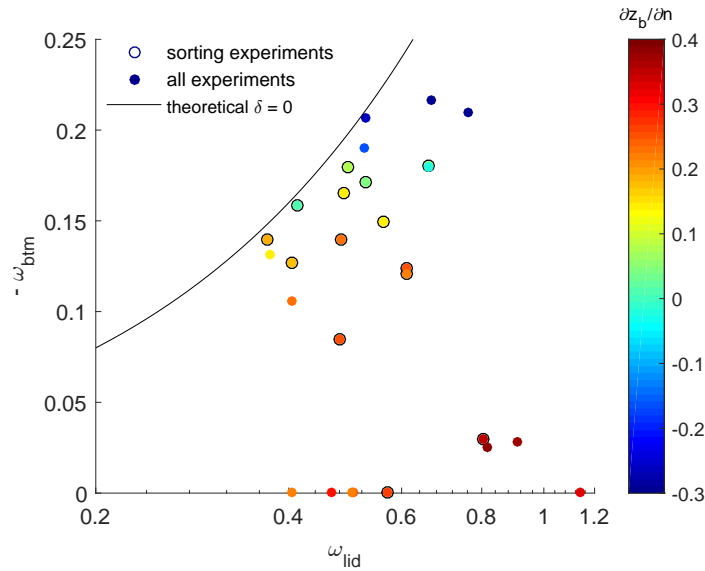


Figure 4.1: Transverse bed slopes for all experiments. The theoretical $\delta = 0$ line is based on eq. 2.22. Sorting experiments were analysed in further detail.

Table 4.1: Flow and morphology-related parameters for the sorting experiments. θ and δ are based on approximations, namely eq. 2.24 in 2.6 and 2.14, and eq. 2.22 respectively.

Experiment	$\partial z_b / \partial n$ [-]	ω_{lid} [rad/s]	ω_{btm} [rad/s]	θ [-]	δ [-]	β [-]	Δ [cm]	λ [m]
20	0.01	0.41	-0.40	0.065	0.005	0.65	0.04	2.84
19	0.04	0.66	-0.18	0.142	0.040	1.07	0.04	0.99
26	0.05	0.53	-0.17	0.098	0.023	0.49	0.03	1.14
32	0.07	0.49	-0.18	0.091	0.011	0.14	0.03	1.27
33	0.15	0.49	-0.17	0.085	0.085	0.12	0.03	1.12
27	0.15	0.56	-0.15	0.101	0.042	0.29	0.05	1.53
28	0.18	0.41	-0.13	0.057	0.026	0.15	0.05	2.21
22	0.22	0.61	-0.12	0.107	0.065	0.29	0.09	2.12
31	0.23	0.48	-0.14	0.078	0.034	0.15	0.06	1.76
34	0.25	0.61	-0.12	0.108	0.064	0.25	0.09	2.12
23	0.26	0.48	-0.08	0.064	0.072	0.28	0.10	0.80
14	0.26	0.57	-0.00	0.065	0.139	0.52	0.09	1.14
21	0.35	0.81	-0.02	0.140	0.128	0.37	0.14	1.70

4.1 Qualitative description of the experiments

Experiments with significant secondary flow started with erosion of the outer bend as sediment was transported net bend inward by secondary currents in small-sized, lobe-shaped bed forms (Figure 4.2). This led to the development of a transverse bed slope, which overshoot before converging to its equilibrium value (Figure 4.3). As the transverse slope formed, the transverse bed slope effect was prompted, causing part of the grains to be diverted toward the outer bend; the stronger the secondary currents, the coarser these outward directed grains were. Over time, the rippled bed forms amalgamated into dunes, leading to longer and often higher bed forms. In case ω_{btm} and ω_{lid} were chosen such that the transverse bed remained near-horizontal, the sediment transported in the outer bend resembled by and large the original mixture.

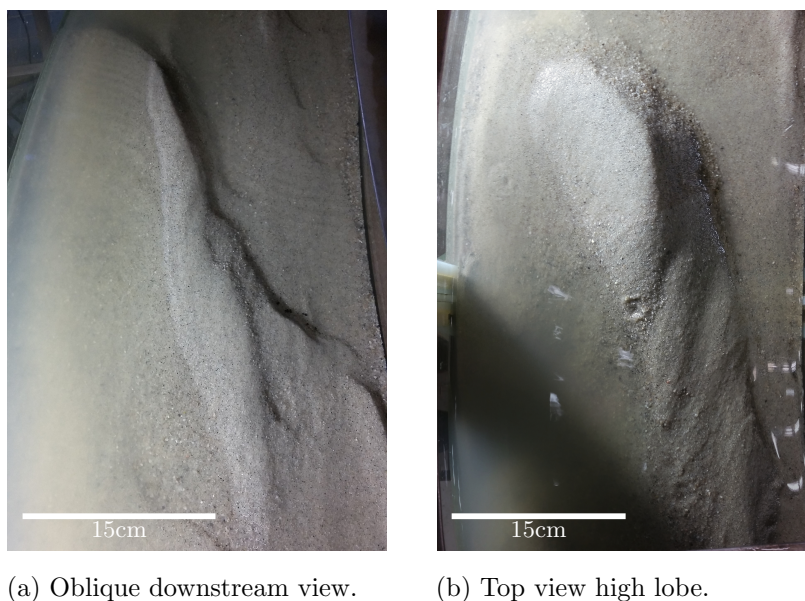


Figure 4.2: Initial bed forms that travelled oblique to the streamwise flow toward the inner bend. The main propagation direction shifted from oblique to streamwise as the transverse bed approached its equilibrium. In both sub figures, flow is toward the top, with the inner bend at the right hand side.

In more detail, the bend inward moving sediment started as a ridge over the entire length of the flume before it broke apart into multiple small-sized, lobe-shaped bed forms. These bed forms formed quicker in experiments with relatively high Shields stress and extended laterally as they moved toward the inner bend. Grain mobility increased in the inner bend once the bed in the inner bend was elevated by accumulating sediment. Lastly, a narrow runnel formed along the inner wall as the transverse slope developed. Predominantly only in experiments with relatively high θ , this narrow, elongated depression was squeezed out.

Typical bed morphology at morphodynamic equilibrium was a transverse bed slope with ripples in the inner bend and dunes in the outer bend (Figure 4.4). Generally, the transverse slope was largest in the dune troughs and smallest at the dune tops. Lateral transport was relatively most pronounced in the dune troughs and appeared nearly absent on the dune tops, especially of long dunes, based on the trajectories of individual grains. So, it seemed that under morphodynamic equilibrium conditions, less than a dune length was required for flow to move the grain sizes to their equilibrium radius after having been entrained in the dune troughs.

The transverse bed slope was convex when near-horizontal, peaking near the channel axis. As the transverse slope increased, it became straight, tending toward a concave profile, meaning that over the lateral, the inner bend was steeper than the outer bend (Figure 4.7).

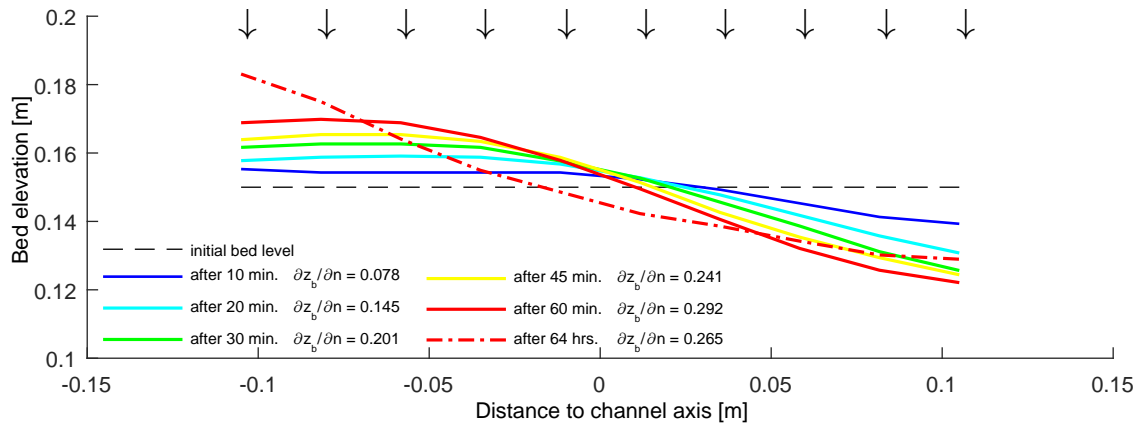


Figure 4.3: Transverse bed slope development. The transverse bed slope overshoots, after which it approaches an equilibrium. The equilibrium slope profile is of experiment 14. The 10 radii scanned with an echosounder (footprint ~ 2 cm) are denoted as arrows. The inner and outer 4.65 cm were left unscanned.

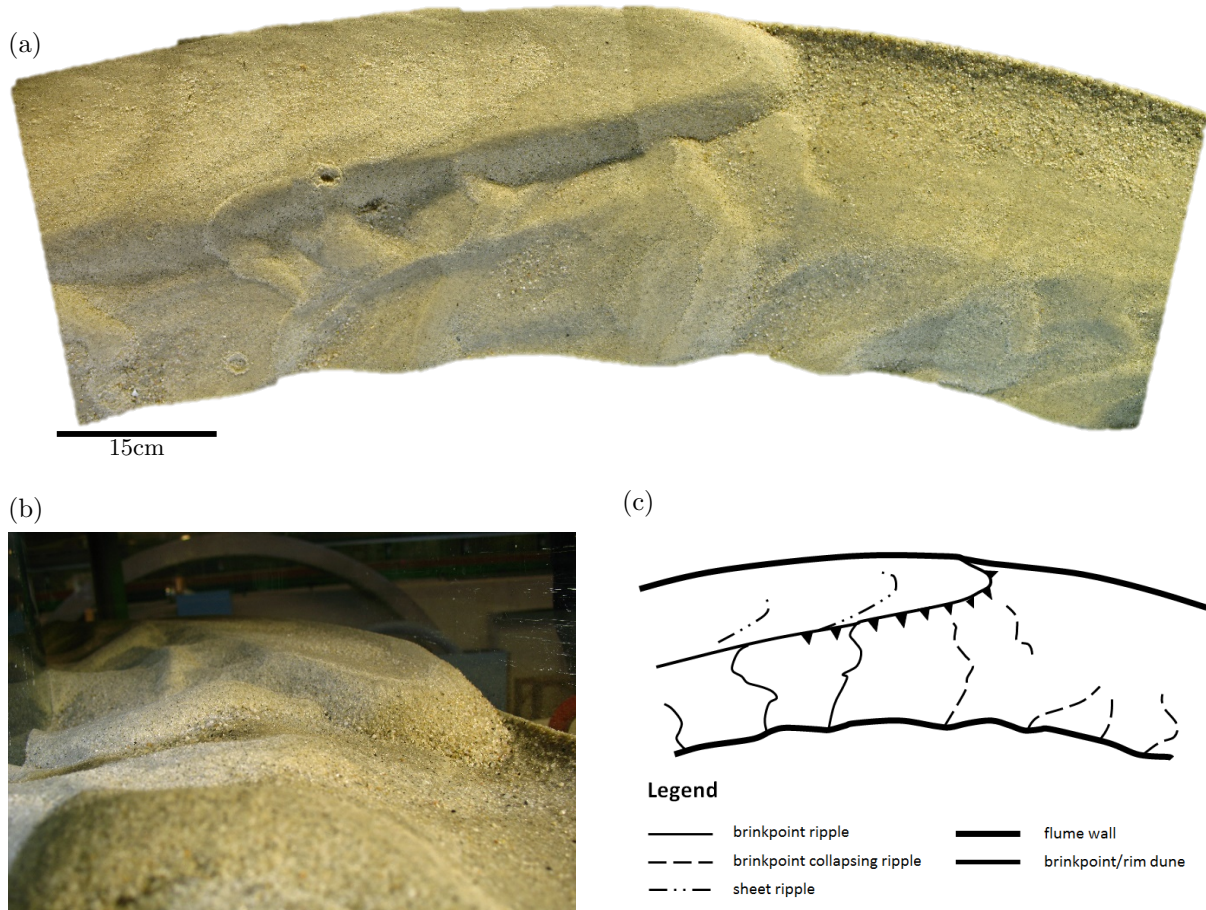


Figure 4.4: Impression of morphology and grain size distribution on a near-horizontal bed (exp. 20). **a)** Top view of a section of the bed in the annular flume. Flow was from left to right, light source is at NNW. In the outer bend, there is a dune top, followed by a coarse trough. In the inner bend are ripples that collapse downstream of the dune's brinkpoint. Craters are caused by drops falling repeatedly from the top lid after drainage. **b)** Upstream directed view. **c)** Schematic interpretation of 4.4a.

Two kinds of ripples were observed: (1) classical ripples with a distinct top and trough (Figure 4.5), and (2) very flat, lobe-shaped ripples, henceforth denoted as sheet ripples (Figure 4.5b). Classical ripples mainly occurred in the narrow, fine-grained runnel in the inner bend in experiments with relatively low sediment mobility. These formed in the dune trough and grew to their equilibrium shape in downstream direction. Widening of the runnel at the dune's brinkpoint caused lateral extension and usually collapse of the ripples, starting the process anew (Figure 4.4a,c). Sheet ripples formed on the dunes in the outer bend. It appeared that the sheet and classical ripples developed in pairs, if both occurred simultaneously. Lastly, tiny, irregular assemblages of medium-to-coarse grains were marked as wavelets.

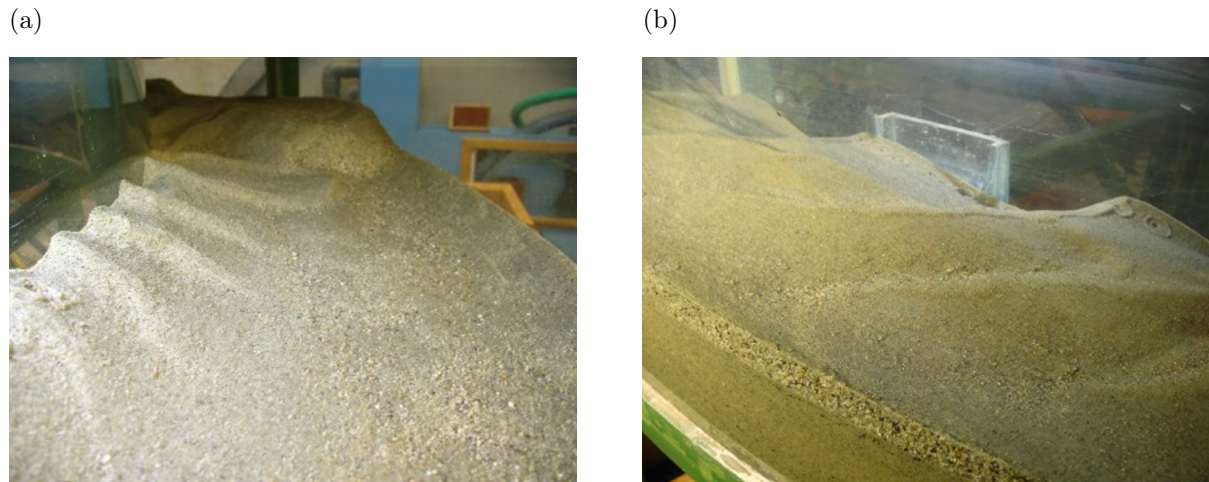


Figure 4.5: **a)** Ripples in the inner bend of an experiment with a near-horizontal slope (exp. 26). View is upstream directed. **b)** Classical ripples in the inner bend (right) and sheet ripples in the outer bend (left) in a near-horizontally sloped experiment (exp. 19). Sheet ripples seemed to be connected to the classical ripples in the inner bend. Flow was from the lower right to the upper left.



Figure 4.6: Well developed bend sorting at lee side of a dune for a steep transverse slope (exp. 22). View is upstream directed. Photo was taken unintentionally at a slight angle, so transverse slope may seem gentler than 0.22.

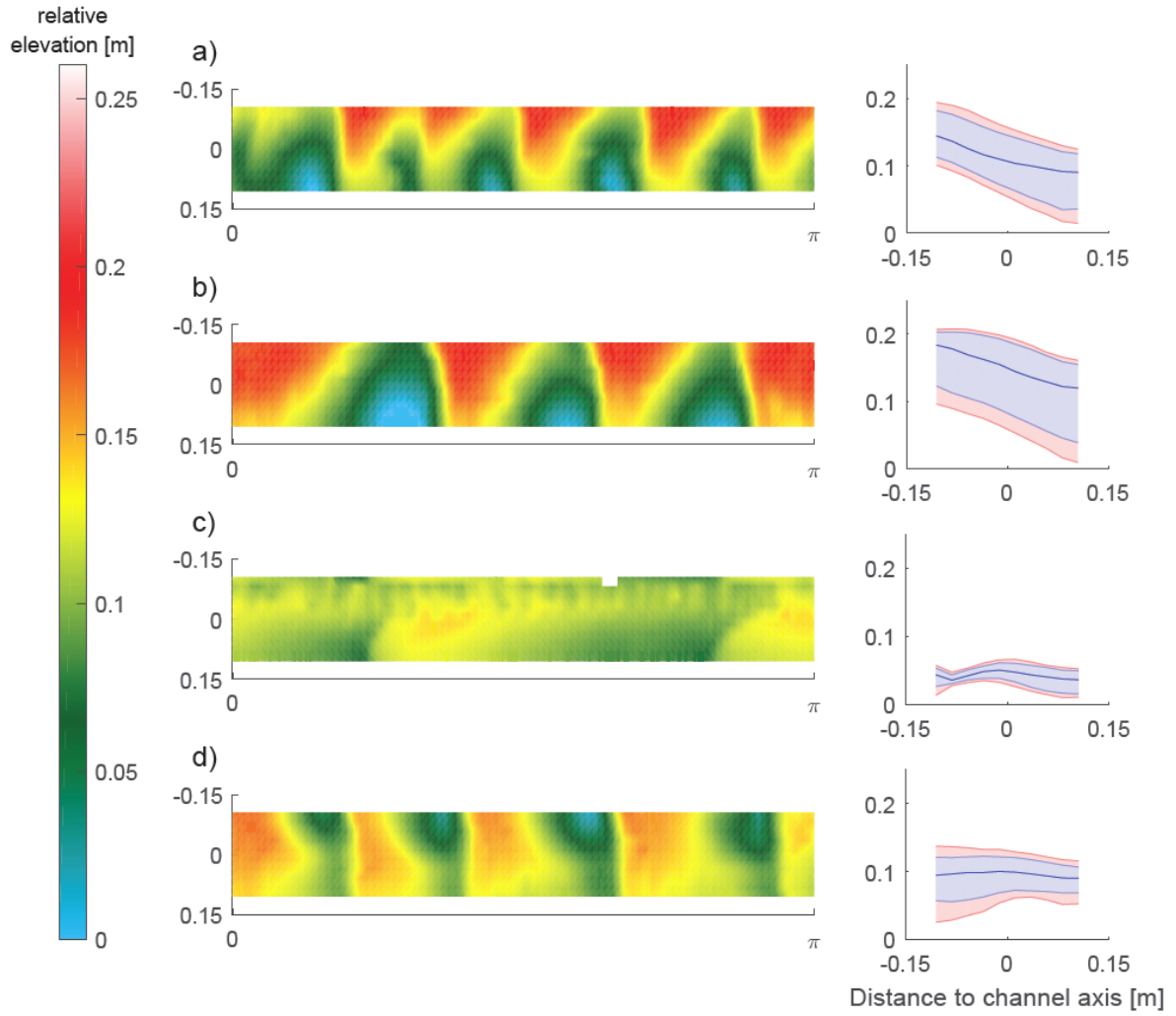


Figure 4.7: Digital elevation models and mean transverse slopes for corners of the measured reach $\partial z_b / \partial n$ and θ / θ_{cr} . Flow is from right to left. **a)** step slope, small mobility (exp. 14); **b)** step slope, high mobility (exp. 21); **c)** near-horizontal slope, small mobility (exp. 20); **d)** near-horizontal slope, high mobility (exp. 19). In the transverse slope plots: blue line is mean transverse slope, blue range is first deviation and red range is second deviation.

4.2 Lateral sorting

4.2.1 Effect of transverse bed slope

There is more distinct lateral sorting with steeper equilibrium transverse slopes (Figures 4.6 - 4.9). This trend is observed for both surface and bulk samples. Generally, the outermost sample is coarsest in cases with significant secondary flow. In few experiments, fine material was deposited adjacent to the flume's outer wall, which thereby reduced the d_{50} of the sample. In such cases, the second sample from the flume's outer wall is coarsest.

Near-horizontal transverse beds show little variation in grain size distributions on the dune top and lee side, in terms of d_{50} and σ . Bulk samples are on average slightly coarser. Although the mean transverse bed slope was close to zero for this $\partial z_b/\partial n$ class, dune troughs locally

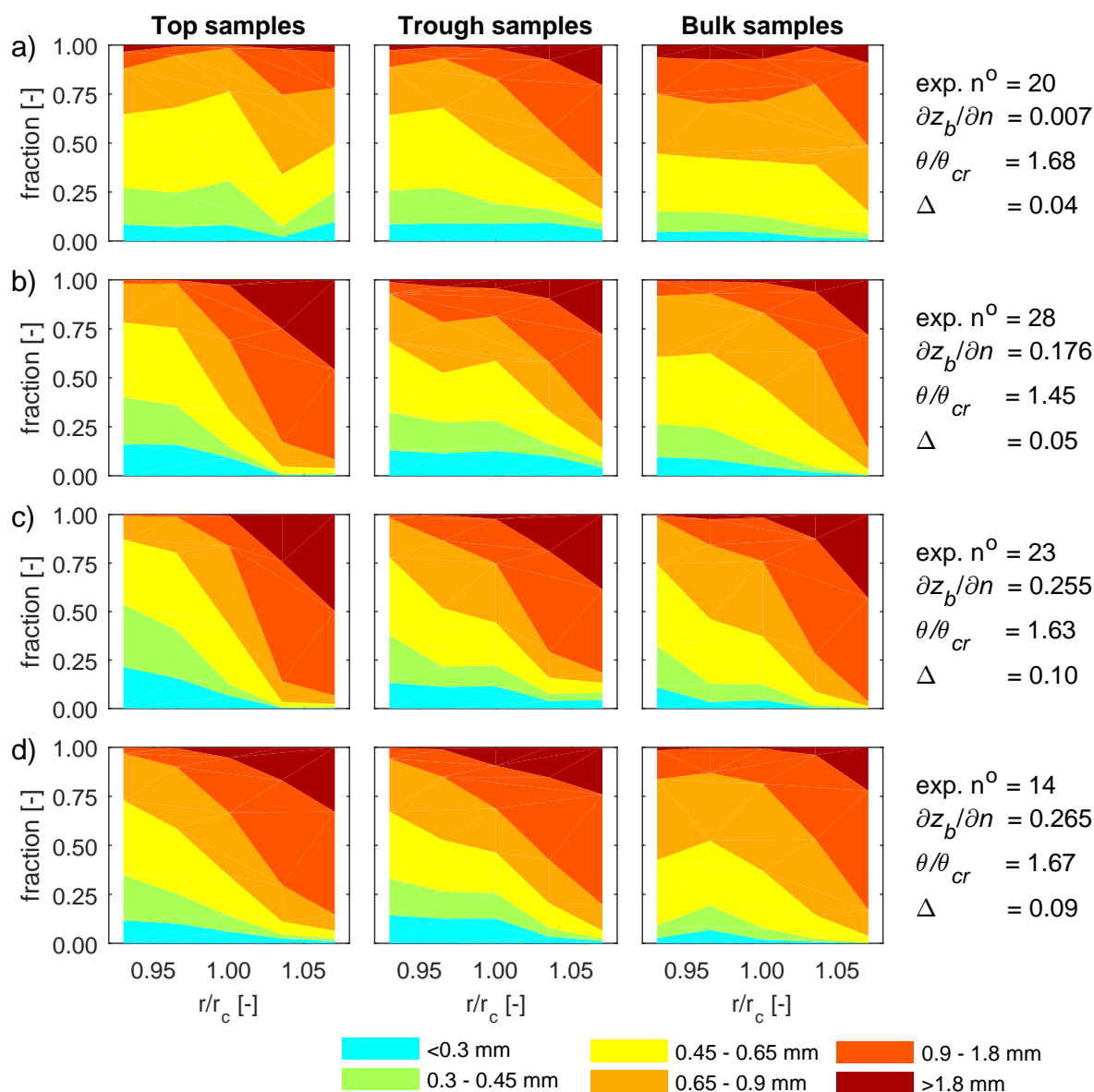


Figure 4.8: Effect of transverse bed slope on lateral sorting for $\theta/\theta_{cr} \sim 1.6$. For increasing transverse bed slope (from a to d), lateral sorting becomes more distinct. Each sample is divided into six grain size classes and samples that were done in twofold are averaged. In each plot, left is the inner bend, right the outer bend.

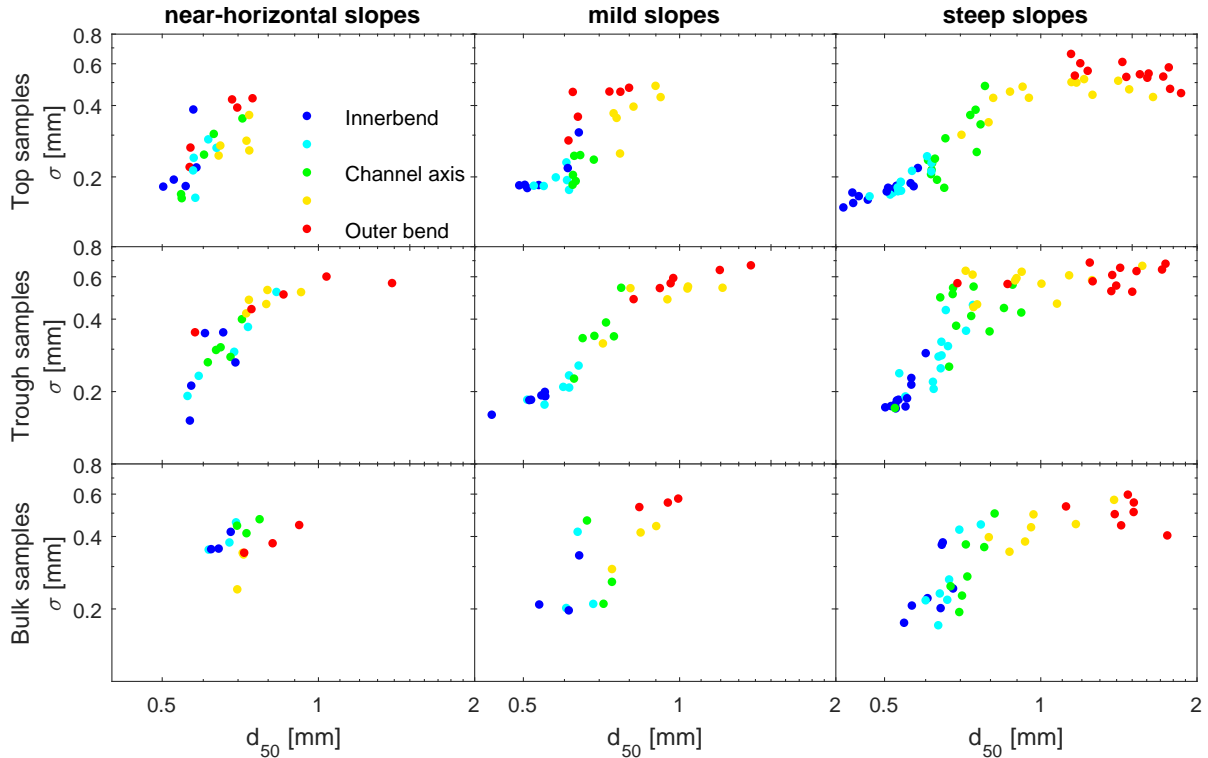


Figure 4.9: Effect of transverse bed slope on lateral sorting, split into three classes: near-horizontal slopes (≤ 0.07), mild slopes ($0.07 - 0.15$) and steep slopes (≥ 0.15). The grain size distributions of all samples is reduced to the median grain size d_{50} and standard deviation σ .

attained transverse slopes up to 0.25, for example in experiment 20; it is at these locations that relatively most lateral variation was present, with d_{50} increasing toward the outer bend (Figure 4.8a).

Mildly sloped transverse beds exhibit distinct lateral sorting in the dune troughs, with high standard deviation and median grain size in the outer bend and low in the inner bend (Figure 4.9). Again, transverse slopes in troughs were considerably steeper than the mean longitudinal transverse slope. The trend of lateral sorting was not seen in the top and bulk samples. Dune height ranged up to 5 cm in this slope class.

Steep slopes concur with clear-cut sorting for both surface and bulk samples, where lateral sorting is most pronounced on the dune tops. Besides the trends being similar to the troughs of mildly sloped experiments, the range of d_{50} extends to even larger values. Typically, $d_{50} > 1$ mm is found for the outer bend. Additionally, dune troughs generally have slightly larger σ values for this range than top and bulk samples.

Table 4.2: Internal variability of lateral sorting. Dune troughs exhibit more variation in lateral sorting in a single experiment than dune tops, especially in the outer bend. Top row r/r_c is inner bend, bottom row r/r_c is outer bend.

r/r_c	median STD tops	median STD troughs	trough/top ratio
0.93	0.0167	0.0203	1.2192
0.96	0.0147	0.0214	1.4576
1.00	0.0201	0.0421	2.0962
1.04	0.0248	0.0459	1.8521
1.07	0.0227	0.0663	2.9196
Mean:	0.0198	0.0392	1.9089

Comparison with the median grain size of the initial mixture $d_{50,in}$ shows that the outer and inner bend become more uniform by lateral sorting (Figure 4.10). Although the absolute σ in the outer bend is fairly large, it is relatively smaller than of the initial mixture. Furthermore, the sediment distribution characteristics (i.e. d_{50} , σ) in the outer bend are most affected by varying degrees of lateral sorting. In contrast, these characteristics in the inner bend are quite constant over the experiments.

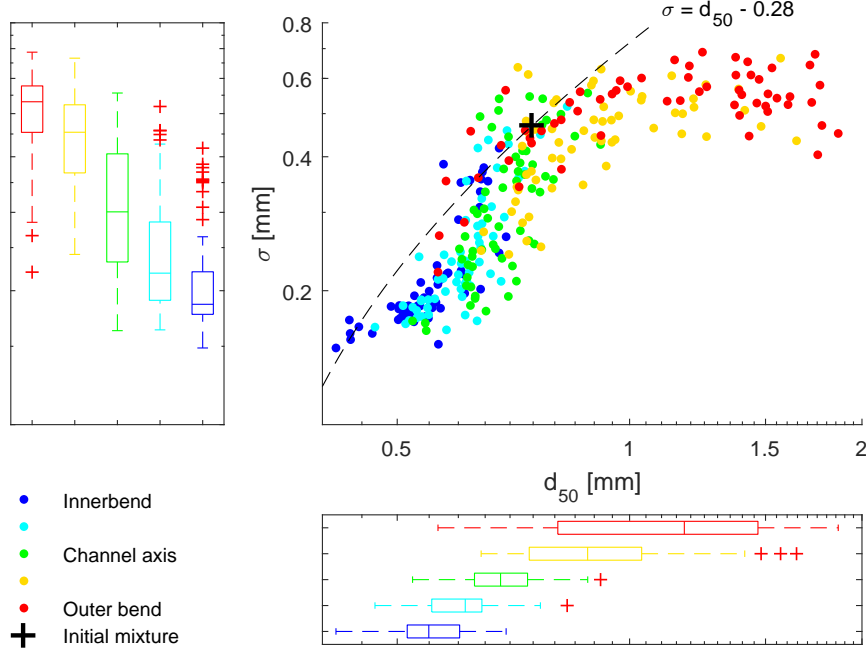


Figure 4.10: Standard deviation versus median grain size for entire data set. The line of equality was positioned over the initial mixture. So, data below this line is more uniform than the initial mixture, which is especially the case for the outermost and innermost sampled radii. The outer bend shows most variation over the experiments in terms of median grain size, the inner bend the least.

Dune troughs exhibit a factor two more variation in lateral sorting than dune tops over the entire lateral reach (Table 4.2); and, it is nearly a factor three when taking into account only the outermost sampled radius. In dune troughs, most internal variability is found for the outermost sampled radius ($r/r_c = 1.07$), while on the dune tops, it is for the second outermost radius ($r/r_c = 1.04$).

Skewness correlates well with d_{50} , yet fails to discriminate sufficiently between the sampled radii (Figure 4.11). Dips in Sk coincide with peaks in the initial sediment mixture at $d_{50} \approx 0.6$ and 1.7 mm. The sediment distribution is typically near-symmetrical around $d_{50} = 0.6$ and 1.2 mm, strongly fine skewed around $d_{50} = 0.8$ mm and strongly coarse skewed at $d_{50} = 1.7$ mm.

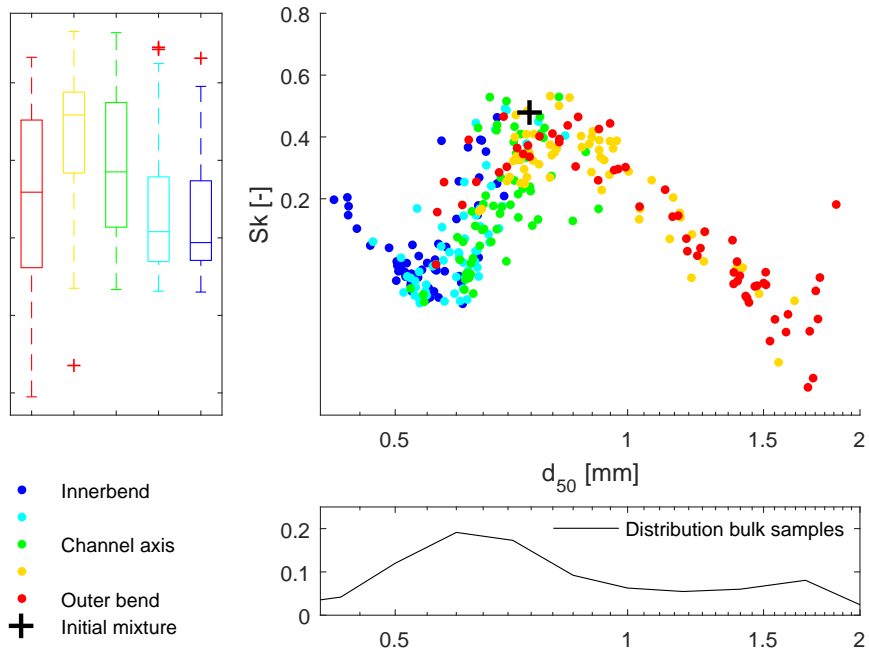


Figure 4.11: Skewness versus median grain size for the entire data set. Skewness correlates well to median grain size, but fails to distinguish between the five sampled radii adequately. Dips in skewness coincide with peaks of the initial sediment distribution.

4.2.2 Effect of sediment mobility

There is a tendency that a smaller sediment mobility leads to more pronounced lateral sorting within the steeply-sloped class (Figure 4.12). Moreover, all radii seem to become more densely clustered; the two outermost sampled radii are relatively coarse and have a large σ – though relatively more uniform than the initial mixture (see section 4.2.1). The innermost radii are very fine and have a small σ . The channel axis wobbles in between, usually resembling the inner bend more (Figure 4.12).

Most pronounced sorting in terms of d_{50} is found on dune tops with low sediment mobility. Distinction between the sampled radii based on σ appears best for dune tops with medium sediment mobility. Peculiarly, the latter is the only trend of sediment mobility with location on dunes that shows a linear trend on the log-log scale (Figure 4.12).

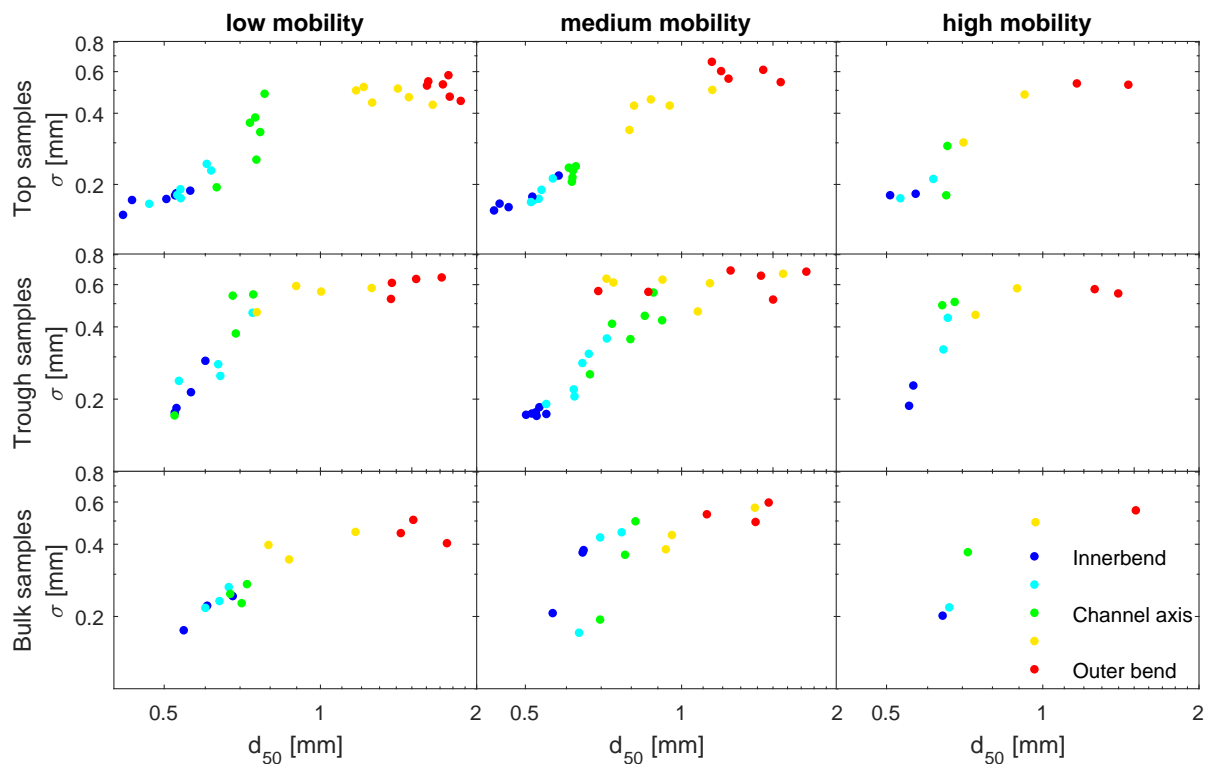


Figure 4.12: Effect of sediment mobility on bend sorting for steeply sloped experiments, split into three classes: low ($\theta/\theta_{cr} \leq 1.5$), medium ($\theta/\theta_{cr} [1.5 - 2.5]$) and high ($\theta/\theta_{cr} \geq 2.5$). Lateral sorting slightly improves with lower sediment mobility for the top samples.

4.3 Bed forms in the carousel flume

The arrangement of ripples in the inner bend and dunes in the outer bend is also identified in the bed form diagram (Figure 4.13); here, samples in the inner bend are bordering on the ripple-dune transition. In contrast, the outer bend is on average at a greater distance from this transition, and is closer to the threshold of motion. The latter is partly caused by the assumption in Figure 4.13 that bed shear stress is equal over the width of the flume.

Dune height increases linearly with smaller $\omega_{btm}/\omega_{lid}$ ratios, given $\partial z_b/\partial n \geq 0$ and $\omega_{btm} < 0$ (Figure 4.14). Also, dunes become higher with steeper transverse slopes, of which the latter parameter depends on $\omega_{btm}/\omega_{lid}$, too. Most dunes fall within a factor two of the maximum dune height possible according to eq. 2.19. The brinkpoints of the dunes were often oblique to the streamwise flow direction (e.g. Figure 4.4). Only for two near-horizontally sloped experiments (exp. 19 & 26) were the dunes' brinkpoints approximately perpendicular to the mean flow direction.

The vertical successions of the inner and outer bend show a fining upward trend (Figure 4.15). In case of near-horizontally sloped experiment 19, the successions are well developed, where the outer bend is only slightly coarser. Broadly, standard deviation increases towards the dune's base. In steeply sloped experiment 34, the inner bend has little vertical variation in d_{50} , whereas the outer bend has considerable. Additionally, standard deviations are substantial for the outer bend, shifting from strongly fine skewed to strongly coarse skewed towards the dune's base, neglecting the uppermost sample.

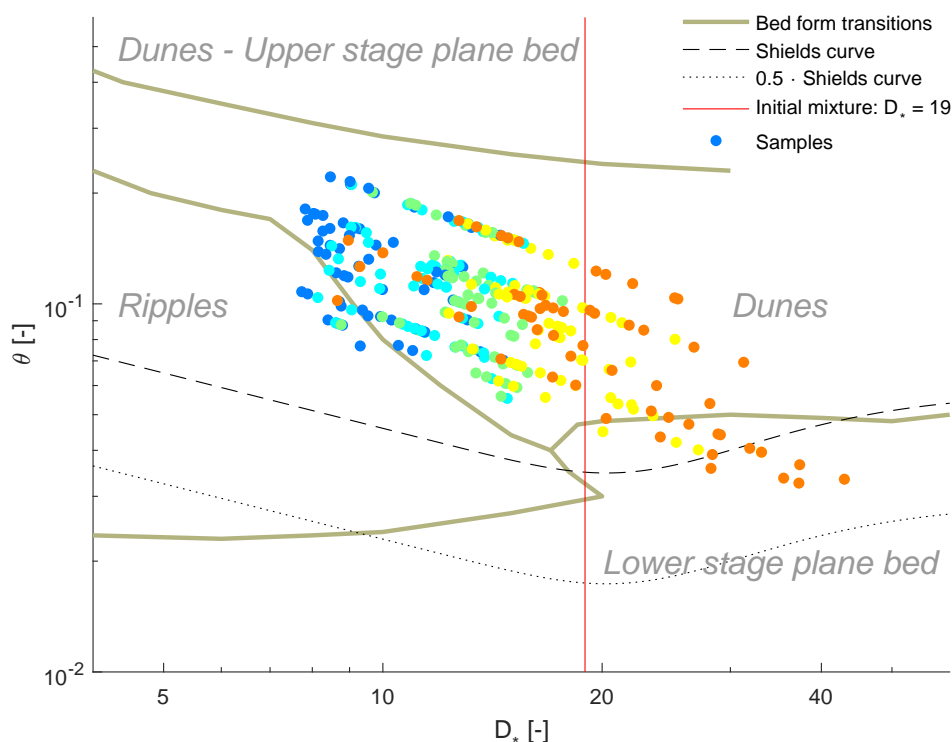


Figure 4.13: Samples in the bed form diagram of Van den Berg and Van Gelder (1993). From blue to red is analogous to from the inner to outer bend. The inner bend borders the ripple-dune transition and it is at this location in the flume that ripples are observed. Due to lateral sorting, the outer bend shifts deeper into the dune regime. In this figure, it is assumed bed shear stress is equal over the width of the flume, which explains the lower sediment mobility for the coarser outer bend. The 'Lowered' Shields curve is a factor 2 lower than the original Shields curve.

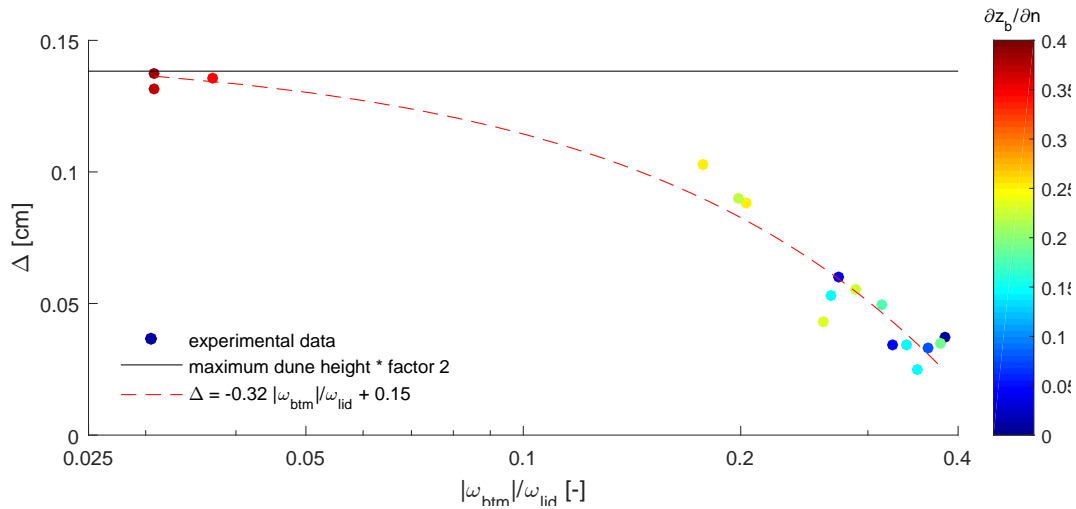


Figure 4.14: Dune height increases linearly with stronger secondary flow, here denoted as the relative rotation speeds of the flume itself versus that of the top lid. Experiments with reverse slopes are excluded in this figure. Furthermore, transverse slope increases with stronger secondary flow, which may also influence dune height.

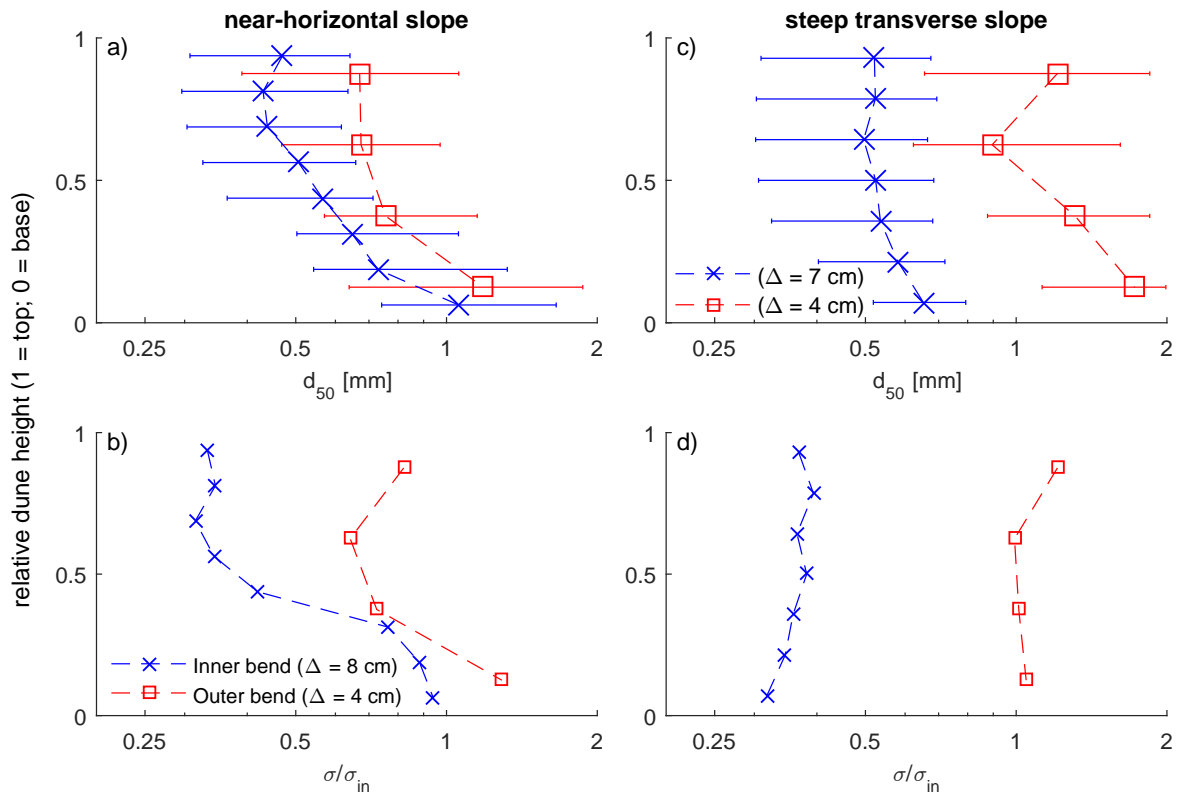


Figure 4.15: Fining upward trend in inner and outer bend of an experiment with a near-horizontal slope (experiment 19) (a & b) and with a steep slope (experiment 34) (c & d). Dune heights are comparable between the experiments. The relatively large standard deviation at the dune's base in the outer dune of b) is caused by accidental inclusion of some finer sediment below the dune's base.

5 Discussion

5.1 Bend sorting in an annular flume

Bend sorting developed in the carousel with a coarser outer bend and finer inner bend when the transverse bed slope was inclined (Figure 4.8), which is in agreement with bend sorting theory and earlier findings in curved flumes (Ikeda et al., 1987; Yen and Lee, 1995; Yen and Lin, 1997), in numerical models (e.g. Parker and Andrews, 1985) and in natural meanders (e.g. Julien and Anthony, 2002; Clayton and Pitlick, 2007). This is caused by the grain size dependence of the transverse bed slope effect and secondary flow (Ikeda et al., 1987); the gravitational pull scales to grain size to the power three, whereas the inward directed drag by secondary flow scales to the square of the grain size. Consequently, coarser grains are pulled down more than fine grains relative to the secondary flow. Moreover, the finer grains in the inner bend create a relatively smooth surface on which coarser grains are pulled down more easily.

The tails of the sediment distribution ended up adjacent to the flume's wall in the inner (fine) and outer bend (coarse), where grain size was uniform than the initial sediment mixture (Figure 4.10). The transition between the inner and outer bend was gradual and less uniform. This implies there is a shift in porosity over the lateral: relatively higher porosity in the inner and outer bend and lower porosity around the channel axis.

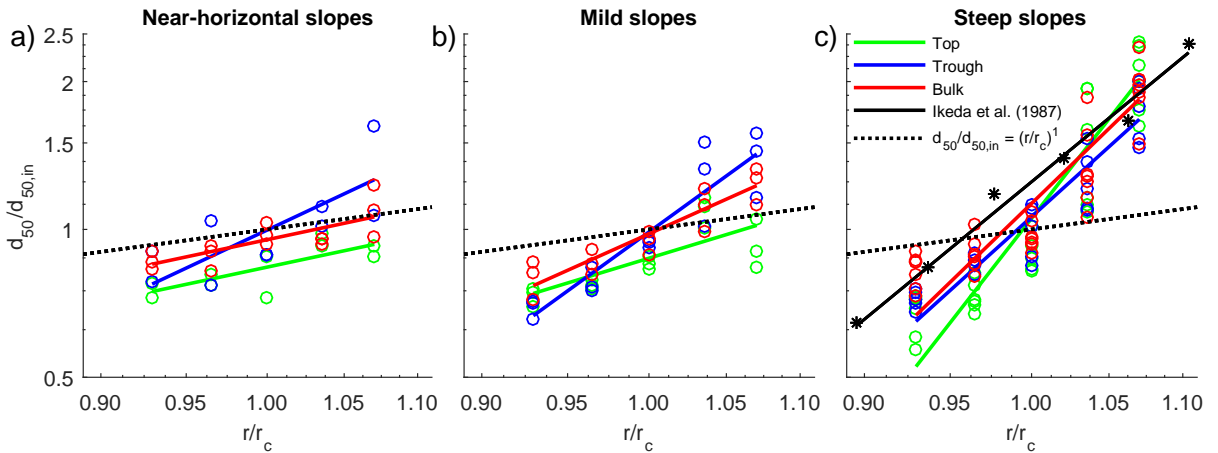


Figure 5.1: Lateral sorting described as $d_{50}/d_{50,in} = a \cdot (r/r_c)^b$ for a) near-horizontal slopes, b) mild slopes and c) steep slopes for the top, trough and bulk samples. The steeper the power regression, the more distinct lateral sorting is. Longitudinal variation in the degree of lateral sorting is seen for the near-horizontal and mild slopes, and partly vanishes for steep slopes. Data of Ikeda et al. (1987) resembles this study's.

Characterising lateral sorting using eq. 2.16 for the steeply sloped class shows fairly good correspondence between this study and Ikeda et al. (1987) (Figure 5.1c). A least-square power fit of the data of Ikeda et al. (1987) was used instead of their predicted curve in Figure 2.6a, because the latter underpredicted median grain size in the inner bend significantly. The empirical parameters for the steeply sloped class of this study, averaged over the three sample locations, are on the order of:

$$\frac{d_{50}}{d_{50,in}} = 1.1 \left(\frac{r}{r_c} \right)^{7.8} \quad (5.1)$$

where the first coefficient (a in eq. 2.16) determines the median grain size averaged over the width, and the power determines the degree of lateral sorting, namely the higher the power, the more distinct sorting is.

It is likely however, that the effect of lateral sorting on the transverse bed slope was significant in the experiment of Ikeda et al. (1987), which may have influenced the equilibrium state. Namely, their sediment mixture was coarse skewed and likely not close to equimobility, which means it is feasible armouring could occur in the outer bend. Furthermore, Ikeda et al. (1987) applied flow conditions that disfavoured bed form formation, which suggests a thin active layer. This could lead to a faster response of lateral sorting compared to the morphological response – in comparison, in this study a thick active layer was present, contributing to relatively fast morphological response. Combined with the (small) possibility of armouring, a relatively fast response of lateral sorting suppresses the development of the maximum attainable equilibrium transverse slope and thereby, the degree of lateral sorting.

Comparison with Yen and Lee (1995) is without use, because samples were taken while the morphology and sorting were still evolving to a new morphodynamic equilibrium. Furthermore, the modality and skewness of the initial mixture are unknown.

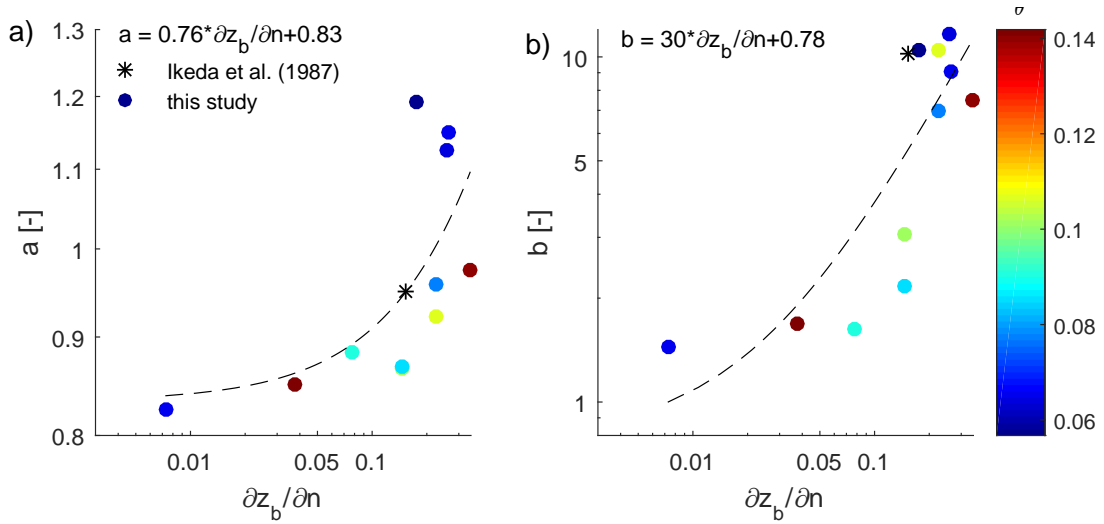


Figure 5.2: Coefficients a) a and b) b in eq. 2.17 as function of transverse slope for the dune tops. The relation of both coefficients with the transverse slope was approached with a linear trend. Data of Ikeda et al. (1987) resembles the trend found in this study. There is no significant relation between either coefficients and sediment mobility.

5.1.1 Effect of the transverse slope

The transverse slope increases with stronger secondary flow (Figure 4.1) and influenced the degree of lateral sorting: lateral sorting is well developed for transverse slopes over 0.15, less for milder slopes and nearly absent for near-horizontal slopes (Figures 4.8, 4.9 & 5.1). The nonlinearity of the gravitational pull and inward directed drag by secondary flow increases, causing increasingly stronger pull-down of coarser grains and stronger up-slope transport of finer grains.

This nonlinear dependence on transverse slope is found on the dune top (Figure 5.2), where eddy turbulence is relatively small and grains had had a long distance to sort, of the form:

$$\frac{d_{50}}{d_{50,in}} = (0.76\partial z_b/\partial n + 0.83) \left(\frac{r}{r_c}\right)^{30\partial z_b/\partial n + 0.78} \quad (5.2)$$

The factor in eq. 5.2 implies that the median grain size taken over the lateral becomes coarser with increasing transverse slope. However, for transverse slopes exceeding 0.15, the

power regression sometimes overpredicts the grain size at the channel axis (and underpredicts in the inner bend). Consequently a factors for such slopes are biased to higher values, leading to the conclusion that the factor is less influenced by transverse slope than eq. 5.2 shows.

Longitudinal variation of lateral sorting due to bed forms

Transverse slope varies on the bed form length scale, being steepest in the dune troughs and most gentle on the dune tops. Since secondary flow intensity affects the transverse bed slope, it is abduced that secondary flow intensity also varies on the bed form length scale. Herein, (skewed) dunes act as obstacles of flow, where highest secondary flow intensity is found in the dune troughs. This is in agreement with earlier findings in a natural river which showed that strong transverse currents can develop in dune troughs if the dunes are skewed with respect to the streamwise flow (Kisling-Moller, 1993).

Dune troughs exhibit most distinct lateral sorting relative to dune tops in near-horizontal and mildly sloped experiments (Figures 4.8a, 4.9 & 5.1a,b). This is, because lateral sorting is positively affected by the transverse slope, which is steepest in dune troughs. However, this 'advantage' of dune troughs having more distinct lateral sorting because they are steeper, fades in the steeply sloped class. It is hypothesised that eddy turbulence in the trough impedes further lateral sorting.

Because dune troughs are generally much steeper than the mean transverse slope, the degree of lateral sorting at these locations cannot be correlated well to the mean transverse slope of an experiment. This is reflected in steeper regressions for near-horizontal and mild slopes compared to the bulk and top samples (Figure 5.1). An improvement that is proposed here, which was not conducted in this study, is to correlate the degree of lateral sorting to the local transverse slope instead of the mean transverse slope. It is hypothesised that after this correction, bend sorting develops more distinct on dune tops than in dune troughs for a given slope due to differences in (eddy) turbulence.

5.1.2 Effect of sediment mobility

The slope parameter β decreases slightly with increasing sediment mobility, resembling the relation of Sekine and Parker (1992) best (Figure 5.3). The relatively weak dependence on sediment mobility suggests that sediment mobility is less important in determining the transverse bed slope (Baar et al., in prep.) than found in most previous studies, assuming that lateral sorting did not affect the equilibrium transverse bed slope considerably in this study. A plausible cause for the strong dependence on sediment mobility found in previous experimental studies (e.g. Struiksma et al., 1985; Ikeda et al., 1987) is that sediment mobility and secondary flow intensity could not be isolated for a given discharge (see section 2.6). So, a steeper transverse bed which is caused by stronger secondary flow is indirectly (and partly incorrectly) coupled to larger sediment mobility in such experiments.

Higher sediment mobility appeared to lead to slightly less pronounced lateral sorting (Figure 4.12). However, this trend is insignificant after further data reduction (Figure 5.2); as long as all sediment is mobile as bed load, lateral sorting is unaffected by sediment mobility. This also shows that the deviation angles $\angle\psi$ of differently sized grains do not heavily depend on sediment mobility, but mainly on grain size, namely on the nonlinearity of gravitational pull-down and up-slope drag by secondary flow.

Only at or just below the threshold of motion is sediment mobility hypothesised to affect lateral sorting, especially in case of wide mixtures. The coarse fraction will be less or immobile, meaning hiding and exposure effects become prominent. This will hamper lateral sorting. Furthermore, an armour layer may form in the outer bend, impeding further transverse slope development. This also negatively affects the degree of lateral sorting.

5.1.3 Effect of lateral sorting on the bed form regime

Two factors likely affect the observed lateral shift in bed form regime, that is, from dunes in the outer bend to ripples in the inner bend (Figures 4.4 & 4.13): lateral sorting and redistribution of flow momentum. The former causes the inner bend to become finer because coarser grains are diverted to the outer bend, which conveys a drop of D_* . Because the D_* of the initial mixture lays close to the ripple-dune transition, a reduction of median grain size in the inner bend swiftly leads to ripples being favoured over dunes. In contrast, the outer bend coarsens and moves away from the ripple-dune transition.

Second, redistribution of momentum in bend flow causes highest and lowest flow velocities to occur in the outer and inner bend, respectively. This lowers sediment mobility in the inner bend, which will contribute the inner bend to move toward the ripple-dune transition, too. This is especially well seen in experiments with near-horizontal transverse slopes where bend sorting is negligible on the dune tops (e.g. experiment 20) (Figure 4.4).

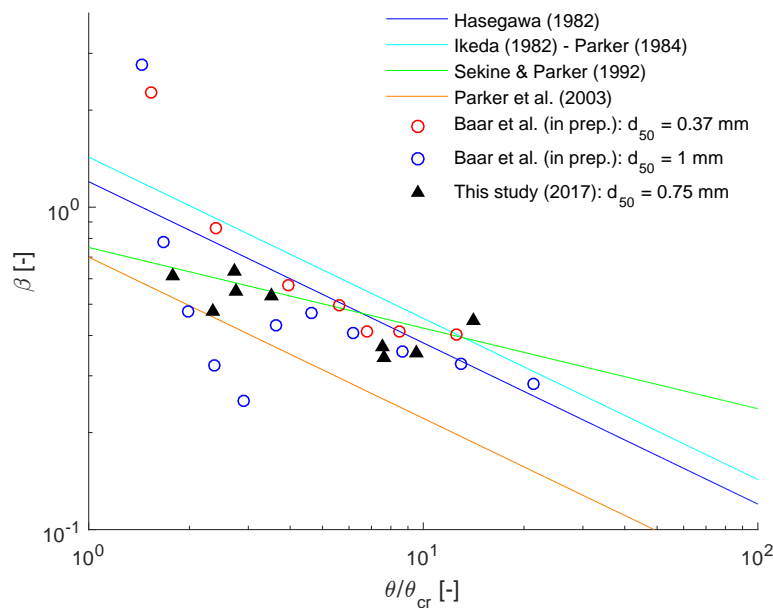


Figure 5.3: Comparison with earlier studies, all showing a net decrease of the slope factor with larger non dimensionalised bed shear stress. This study resembles the findings of [Sekine and Parker \(1992\)](#) best. Counter-rotation of the flume was zero.

5.2 Implications for natural rivers

The annular flume allows measurement of the degree of lateral sorting under constant bend curvature and equilibrium flow conditions. So, the findings of this study provide an indication for the maximum attainable degree of lateral sorting in natural river bends for given flow conditions.

Natural river bend curvature however, is far from constant, which causes variability of lateral sorting in longitudinal direction (Dietrich and Whiting, 1989; Julien and Anthony, 2002). In order to attain well developed lateral sorting in a bend, the following two preconditions must be met: (1) strong secondary flow is directed toward the same riverside for quite a distance, because the transverse slope (Struiksmma et al., 1985) and coupled lateral sorting take time and therefore distance to develop, and (2) all sediment is mobile, so armour layer formation is unlikely.

Sinuosity affects secondary flow intensity: a higher sinuosity usually conveys a decrease in the bend radius relative to the water depth, which in turn leads to stronger secondary flow (eq. 2.8). High sinuosity is generally found in meandering and sinuous rivers. Though, individual channels in a braided river network can make sharp curves as well, such as in the Rakaia River (NZ) (Figure 5.4). Assumed all grains are mobile under average flow conditions, most pronounced bend sorting is expected at or just downstream of a meander apex (Figure 2.4).

River bends of both sand bed (Bridge and Jarvis, 1976 in Clayton and Pitlick, 2007; Dietrich and Smith, 1983) and gravel bed rivers (Clayton and Pitlick, 2007) can develop bend sorting. However, whether distinct bend sorting may develop depends on the discharge required for all grains to be mobile. In threshold channels for example, bankfull discharge or larger is needed to mobilise all grain sizes. Under such conditions, flow is expected to unbend since most bars are flooded, contributing to lower secondary flow intensity and less distinct sorting. In meandering and sinuous rivers on the other hand, chances are greater that a discharge lower than bankfull will mobilise all grain sizes, making such rivers on average more favourable for distinct bend sorting. Furthermore, the direction of secondary flow close to the bed swaps less frequent in long meanders than in braided rivers with small bars, which also implies that most distinct sorting can develop in the former.



Figure 5.4: Fairly sharp river bend in braided river network, Rakaia River (NZ). Flow is from top to bottom. Distinct sorting may develop in the lower-right corner of the contoured section based on the sinuosity. Though, since this is a gravel bed river, grains are generally only mobile for bankfull or larger discharges. Consequently, bend sorting will be poorly developed, also due to unbending of flow. (Google Earth imagery, accessed January 2017)

Hiding and exposure effects will be most prominent in rivers with wide sediment distributions, including sand-gravel bed rivers such as the Allier (FR). Furthermore, due to the wide and/or bimodal nature of the sediment mixture, (extensive) armour layers may develop at inflections (Kleinhans, 2002) and in their river bends and at inflections.

Skewed dunes can contribute to strong transverse currents in the dune troughs (Kisling-Moller, 1993). In the carousel flume, the effect of these currents were also observed, which were directed bend inward, contributing to more pronounced sorting in the dune troughs. In the Gelsa (DK), a sand bed meandering river, corkscrew flow induced by skewed dunes were also directed bend inward, but its intensity varied strongly spatially. Although it is unclear how much corkscrew flow by these dunes influence bend sorting on the natural river scale, its effect is probably greatest in sand bed and mixed sand-gravel bed rivers, since sand organises quicker in dunes than gravel for given flow conditions (Kleinhans, 2002).

So, most pronounced bend sorting is expected in sand-bed rivers with high sinuosity. For example, the Mississippi River at Aitkin County (USA). Least pronounced sorting is hypothesised in gravel-bed and sand-gravel-bed rivers with low sinuosity, for example the Rakaia River (NZ).

6 Conclusions

Experiments were conducted in a rotating annular flume, which allowed the isolation of the effect of transverse bed slope and sediment mobility on the degree of bend sorting. It was found that bend sorting develops when the transverse bed is inclined, with a coarser outer bend and finer inner bend. Additionally, bend sorting becomes more pronounced with steeper transverse slope: well developed for transverse slopes over 0.15 and significantly less distinct for gentler slopes.

The degree of lateral sorting depends on how the gravitational pull-down of grains, which scales to the cube of grain size, compares to the up-slope directed drag by secondary flow, which scales to the square of grain size. This nonlinearity causes coarser grains to be diverted to the outer bend and finer grains to the inner bend. The degree of lateral sorting also influences the fining upward trend in dunes: the fining upward trend in the outer bend is significantly coarser than the inner bend once lateral sorting is well developed. For near-horizontal slopes, differences between the fining upward trend in the inner and outer bend are relatively small.

Higher sediment mobility resulted in a modest increase of transverse bed slope. This opposes most previous research that found a much stronger dependence on sediment mobility. Furthermore, sediment mobility is insignificant in affecting the degree of lateral sorting as long as all grains are mobile as bed load. This opposes my third hypothesis. Only at or just below the threshold of motion is sediment mobility hypothesised to (negatively) affect lateral sorting as hiding and exposure effects become prominent.

Longitudinal variation in transverse bed slope is observed on the bed form length scale, where slopes are steepest in the dune troughs and most gentle on the dune tops. It is abduced that the dunes in the carousel cause longitudinal variation of secondary flow intensity, the latter being highest in the dune troughs. Consequently, bend sorting can develop in dune troughs for gentler mean transverse slopes than on dune tops. This 'advantage' of dunes exhibiting most distinct sorting fades away for mean transverse slopes over 0.15. Eddy turbulence is hypothesised to impede further lateral sorting.

7 Future research

In this chapter, a few ideas are presented to elaborate on, following the experiments in an annular flume of this study.

7.1 Hiding and exposure effects

Hiding and exposure effects were argued to influence the development of the transverse bed slope and bend sorting; for example, exclusion of these effects led to overestimation of the inner bend elevation ([Fischer-Antze et al., 2009](#)). Furthermore, an armour layer may form when the coarser grains end up in the outer bend, hampering further transverse slope development and bend sorting, especially for sediment mobility close to the threshold of motion.

Unfortunately, these concepts were very poorly investigated in previous research. Also in this study, hiding and exposure effects were mitigated due to selection of a small sediment mixture. It is therefore proposed to conduct (1) experiments with a wide sediment mixture – and/or a 'mathematical' mixture with three grain sizes – and (2) take sediment samples and measure flow conditions in natural sand-gravel bed rivers with high sinuosity, where hiding and exposure effects are believed most prominent. It is hypothesised that hiding and exposure lead to gentler transverse bed slopes and less distinct sorting. This implies a shallower thalweg as well.

7.2 Corkscrew currents due to skewed dunes

In the carousel flume, dunes caused considerable longitudinal variation of secondary flow intensity on the bed form length scale which was also observed in a natural river bend ([Kisling-Moller, 1993](#)). In this study it was found that this longitudinal variation influenced bend sorting considerably. However, it is unknown to what extent bed form induced corkscrew currents contribute to lateral sorting in natural river bends. This too, requires fieldwork to provide further understanding.

Acknowledgements

First and foremost, I would like to thank my supervisors Maarten Kleinhans and Anne Baar for their professional guidance, critical thinking and unlimited enthusiasm throughout my research. I am grateful to the technical staff at TU Delft, who acted swiftly whenever the annular flume or measurement equipment decided to break down. I would also like to thank my fellow MSc students Laura Coumou, Lisanne Jagt, Erik van Onselen and Bente de Vries for the enlightening lunch discussions and moral support. Finally, I thank my parents for always supporting me in every decision I make.

References

- Baar, A. W. (in prep.). et al.
- Blanckaert, K. (2011). Hydrodynamic processes in sharp meander bends and their morphological implications. *Journal of Geophysical Research: Earth Surface*, 116(F1).
- Booij, R. (1994). Communications on hydraulic and geotechnical engineering. Measurements of the flow field in a rotating annular flume. *Report no. 94-2*.
- Booij, R. and Uijtewaal, W. S. J. (1999). Modelling of the flow in rotating annular flumes. *Engineering Turbulence Modelling and Experiments*, 4:339–348.
- Bridge, J. S. (1992). A revised model for water flow, sediment transport, bed topography and grain size sorting in natural river bends. *Water Resources Research*, 28(4):999–1013.
- Bridge, J. S. and Jarvis, J. (1976). Flow and sedimentary processes in the meandering river South Esk, Glen Clova, Scotland. *Earth Surface Processes and Landforms*, 1(4):303–336.
- Clayton, J. A. and Pitlick, J. (2007). Spatial and temporal variations in bed load transport intensity in a gravel bed river bend. *Water Resources Research*, 43(2):W02426.
- Dietrich, W. E. and Smith, J. D. (1983). Influence of the point bar on flow through curved channels. *Water Resources Research*, 19(5):1173–1192.
- Dietrich, W. E. and Whiting, P. (1989). Boundary shear stress and sediment transport in river meanders of sand and gravel. *River Meandering*. p. 1–50.
- Engelund, F. (1974). Flow and bed topography in channel bends. *Journal of the Hydraulics Division*, 100(Proc. Paper 10963):1631–1648.
- Engelund, F. (1975). Instability of flow in a curved alluvial channel. *Journal of the Fluid Mechanics*, 72(01):145–160.
- Engelund, F. (1981). The motion of sediment particles on an inclined bed. *Progress Rep*, 53.
- Engelund, F. and Fredsoe, J. (1982). Hydraulic theory of alluvial rivers. *Advances in Hydros-cience*, Academic Press, New York, NY(USA), 13:187–215.
- Fischer-Antze, T., Ruther, N., Olsen, N. R., and Gutknecht, D. (2009). Three-dimensional (3d) modeling of non-uniform sediment transport in a channel bend with unsteady flow. *Journal of Hydraulic Research*, 47(5):670–675.
- Gruijters, S. H. L. L., Veldkamp, J. G., Gunnink, J., and Bosch, J. H. A. (2001). De lithologische en sedimentologische opbouw van de ondergrond van de Pannerdensche Kop. TNONITG report NITG, 01-166 . (in Dutch). *English translation: The lithological and sedimentological composition of the subsoil of the Pannerden's Head*.
- Hasegawa, K. (1981). Bank-erosion discharge based on a non-equilibrium theory. *Proceedings of the Japan Society of Civil Engineers*, 316:37–52. (in Japanese). Japan Society of Civil Engineers.

- Ikeda, S. (1982). Lateral bed load transport on side slopes. *Journal of the Hydraulics Division*, 108(11):1369–1373.
- Ikeda, S. (1989). Sediment transport and sorting at bends. *River Meandering*. p. 103–125.
- Ikeda, S. and Nishimura, T. (1985). Bed topography in bends of sand-silt rivers. *Journal of Hydraulic Engineering*, 111(11):1397–1410.
- Ikeda, S., Yamasaka, M., and Chiyoda, M. (1986). Bed topography and sorting in bends. 埼玉大学工学部建設系研究報告, 16:1–14. (in Japanese).
- Ikeda, S., Yamasaka, M., and Chiyoda, M. (1987). Bed topography and sorting in bends. *Journal of Hydraulic Engineering*, 113(2):190–204.
- Jackson, R. G. (1975). Velocity-bed form-texture pattern of meander bends in the Lower Wabash River of Illinois and Indiana. *Geological Society of America Bulletin*, 86(11):1511–1522.
- Julien, P. Y. and Anthony, D. J. (2002). Bed load motion and grain sorting in a meandering stream. *Journal of Hydraulic Research*, 40(2):125–133.
- Kikkawa, H., Ikeda, S., and Kitagawa, A. (1976). Flow and bed topography in curved open channels. *Journal of the Hydraulics Division*, 120(ASCE 12416).
- Kisling-Moller, J. (1993). Bedform migration and related sediment transport in a meander bend. *Special Publications of the International Association of Sedimentology 17*. p. 51–61.
- Kleinhans, M. G. (2002). Sorting out sand and gravel: sediment transport and deposition in sand-gravel bed rivers. (Doctorial dissertation).
- Kleinhans, M. G. (2004). Sorting in grain flows at the lee side of dunes. *Earth-Science Reviews*, 65(1):75–102.
- Kleinhans, M. G. (2005a). Flow discharge and sediment transport models for estimating a minimum timescale of hydrological activity and channel and delta formation on Mars. *Journal of Geophysical Research: Planets*, 110(E12).
- Kleinhans, M. G. (2005b). Grain-size sorting in grainflows at the lee side of deltas. *Sedimentology*, 52(2):291–311.
- Kleinhans, M. G. (2005c). Upstream sediment input effects on experimental dune trough scour in sediment mixtures. *Journal of Geophysical Research: Earth Surface*, 110(F4).
- Kleinhans, M. G. and Van den Berg, J. H. (2011). River channel and bar patterns explained and predicted by an empirical and a physics-based method. *Earth Surface Processes and Landforms*, 36(6):721–738.
- Kleinhans, M. G. and Van Rijn, L. C. (2002). Stochastic prediction of sediment transport in sand-gravel bed rivers. *Journal of Hydraulic Engineering*, 128(4):412–425.
- Koch, F. G. and Flokstra, C. (1980). Bed level computations for curved alluvial channels: prepared for the 19th IAHR congress, New Delhi, India, February 1981. *Waterloopkundig Laboratorium*.
- Leopold, L. B. and Wolman, M. G. (1957). River channel patterns: braided, meandering, and straight. US Government Printing Office.
- Meyer-Peter, E. and Mueller, R. (1948). Formulas for bed-load transport. IAHR.

- Mueller, E. R., Pitlick, J., and Nelson, J. M. (2005). Variation in the reference Shields stress for bed load transport in gravel-bed streams and rivers. *Water Resources Research*, 41(4):W04006.
- NEDECO (1959). *River studies and Recommendations on Improvement of Niger and Benue*. North Holland Publishing Company.
- Odgaard, A. J. (1981). Transverse bed slope in alluvial channel bends. *Journal of the Hydraulics Division, Proceedings of the American Society of Civil Engineers*, 107(HY12):W02426.
- Odgaard, A. J. (1986). Meander flow model. I: Development. *Journal of Hydraulics Engineering*, 112(12):1117–1135.
- Odgaard, A. J. (1987). Streambank erosion along two rivers in Iowa. *Water Resources Research*, 23(7):1225–1236.
- Olesen, K. W. (1987). *Bed topography in shallow river bends*. Delft University of Technology, Faculty of Civil Engineering.
- Oreskes, N., Schrader-Frechette, K., and Belitz, K. (1994). Verification, validation and confirmation of numerical models in the earth sciences. *Science*, 263(5147):641–646.
- Parker, G. (1984). Discussion of "Lateral bed load transport on side slopes" by Syunsuke Ikeda (November, 1982)". *Journal of Hydraulic Engineering*, 110(2):197–199.
- Parker, G. and Andrews, E. D. (1985). Sorting of bed load sediment by flow in meander bends. *Water Resources Research*, 21(9):1361–1373.
- Parker, G., Seminara, G., and Solari, L. (2003). Bed load at low Shields stress on arbitrarily sloping beds: Alternative entrainment formulation. *Water resources research*, 39(7).
- Rozowskii, I. L. (1961). Flow of water in bends of open channels. Israel Program for Scientific Translation, Jerusalem, Israel. 233 pp.
- Ruther, N. and Olsen, N. R. B. (2005). Three-dimensional modeling of sediment transport in a narrow 90° channel bend. *Journal of Hydraulic Engineering*, 131(10):917–920.
- Schuurman, F. and Kleinhans, M. G. (2013). Major bed slope effects affecting all river morphodynamics models.
- Schuurman, F., Marra, W. A., and Kleinhans, M. G. (2013). Physics-based modeling of large braided sand-bed rivers: Bar pattern formation, dynamics, and sensitivity. *Journal of Geophysical Research: Earth Surface*, 118(4):2509–2527.
- Sekine, M. and Parker, G. (1992). Bed-load transport on transverse slope. I. *Journal of Hydraulic Engineering*, 118(4):513–535.
- Silberman, E., Carter, R., Einstein, H. A., Hinds, J., and Powell, R. W. (1963). Friction factors in open channels. *Journal of the Hydraulics Division, ASCE*, 89(2):97–143.
- Sloff, C. J., Jagers, H. R. A., Kitamura, Y., and Kitamura, P. (2001). 2D Morphodynamic modelling with graded sediment. *Proceedings of the Second IAHR Symposium, River, Coastal and Estuarine Morphodynamics*. 10–14 Sept. 2001, Obihiro, Japan, p. 535–544.
- Sloff, K. and Mosselman, E. (2012). Bifurcation modelling in a meandering gravel-sand bed river. *Earth Surface Processes and Landforms*, 37(14):1556–1566.

- Struiksmā, N., Olesen, K. W., Flokstra, C., and De Vriend, H. J. (1985). Bed deformation in curved alluvial channels. *Journal of Hydraulic Research*, 23(1):57–79.
- Talmon, A. M., Struiksmā, N., and Van Mierlo, M. C. L. M. (1995). Laboratory measurements of the direction of sediment transport on transverse alluvial-bed slopes. *Journal of Hydraulic Research*, 33(4):495–517.
- Talmon, A. M. and Wiesemann, J. U. (2006). Influence of grain size on the direction of bed-load transport on transverse sloping beds. *Third International Conference on Scour and Erosion*. p. 632–639.
- Thorne, C. R., Zevenbergen, L. W., Pitlick, J. C., Rais, S., Bradley, J. B., and Julien, P. (1985). Direct measurements of secondary currents in a meandering sand-bed river. *Nature*, 315(6022):746–747.
- Van Bendegom, L. (1947). Eenige beschouwingen over riviermorfologie en rivierverbetering. *De Ingenieur*, 59(4):B1–11. (in Dutch). *English translation: Some considerations on river morphology and river improvement*.
- Van den Berg, J. H. and Van Gelder, A. (1993). A new bedform stability diagram, with emphasis on the transition of ripples to plane bed in flows over fine sand and silt. *Alluvial Sedimentation (Special Publication 17 of the IAS)*, 17:11–21.
- Van den Bosch, L. (2003). Influence of vegetation on flow and morphology in the river Allier, France. *Doctoral dissertation, TU Delft, Delft University of Technology*.
- Van Rijn, L. C. (1984a). Sediment transport, part I: Bed load transport. *Journal of Hydraulic Engineering*, 110(10):1431–1456.
- Van Rijn, L. C. (1984b). Sediment transport, part III: Bed forms and alluvial roughness. *Journal of Hydraulic Engineering*, 110(12):1733–1754.
- Wiesemann, J. U., Mewis, P., and Zanke, U. C. E. (2006). Downslope transport (transverse sediment transport). *Third Chinese-German Joint Symposium on Coastal and Ocean Engineering*.
- Yen, C. L. and Lee, K. T. (1995). Bed topography and sediment sorting in channel bend with unsteady flow. *Journal of Hydraulic Engineering*, 121(8):591–599.
- Yen, C. L. and Lin, Y. L. (1997). Variations of bed surface sediment size in a channel bend. In *The Interactions Between Sediments and Water*. Springer Netherlands. p. 81–88.
- Zimmerman, C. (1977). Roughness effects on the flow direction near curved stream beds. *Journal of Hydraulic Research*, 15(1):73–85.

Nomenclature

Δ	Bed form height
Λ	Meander wavelength (in Figure 2.3a)
Φ	Friction angle (in Engelund, 1974)
α	Transverse slope (in Van Bendegom, 1947)
β	Slope factor
γ	Ratio of lift force to drag force
δ	Deviation angle of sediment transport by secondary currents, measured in the horizontal plane
ε	Eddy viscosity
ζ	Ratio of projected surface area to volume for a sediment particle normalised by that of a sphere
θ	Dimensionless bed shear stress (= Shields stress)
θ'	Skin friction related dimensionless bed shear stress
θ_{cr}	Critical dimensionless bed shear stress
θ_0	Ratio of dynamic granular friction and fluid drag
$\theta_{cr,0}$	Critical dimensionless bed shear stress on a near-horizontal bed
κ	Von Karman's constant
λ	Bed form length
λ_{he}	Sheltering coefficient (in Parker et al. (2003))
λ_s, λ_w	Adaptation lengths of the bed and main flow to disturbances
μ_d, μ_s	Dynamic and static Coulomb friction coefficient
ν	Kinematic viscosity
ρ, ρ_s	Density of water and sand
$\sigma (\sigma_{in})$	(Initial) inclusive standard deviation
τ	Total bed shear stress
τ'	Skin friction related bed shear stress
$\omega_{btm}, \omega_{lid}$	Rotation velocities of flume and lid
ψ	Net deviation angle of sediment transport on a transverse slope
A_{1-5}, A_s	Calibration factors in eq. 2.23 and 2.24
A_r	Numerical constant (Kikkawa et al., 1976; Ikeda et al., 1987) (Table 2.1)
A_{sh}, D_{sh}	Calibration factors (Sloff et al., 2001) (Table 2.2)
B	- Non dimensional cross sectional area over the width - Channel width (in Figure 2.3a)
C	Chezy parameter
C'	Chezy parameter related to skin friction
D_*	Dimensionless grain size
$F_{*,cr}$	Particle densimetric Froude number based on $\overline{u_{cr}}$
K	Parameter determining the deviation of bed shear stress due to secondary flow
Q_f	Peak discharge (in Figure 2.6)
R_h	Hydraulic radius

S, S_n	Maximum and transverse local water surface slope
$Sk (Sk_{in})$	(Initial) inclusive skewness
T	Transport stage parameter
W	Channel or flume width
a, b	Calibration factors in eq. 2.16
a_2, b_2, c_2	Calibration factor in eq. 2.17
a_β, b_β	Calibration factors in eq. 2.15
c	Constant to accommodate bed form properties
d_x	x^{th} grain size percentile of the mass frequency distribution (e.g. d_{50})
$d_{x,in}$	x^{th} grain size percentile of the mass frequency distribution of the initial sediment mixture (e.g. $d_{50,in}$)
f, f_g	Darcy-Weisbach friction factor related to the sediment and to the glass side-walls of a flume
g	Gravitational constant
h, \bar{h}	Local and mean water depth
k_s	Nikuradse roughness length
q_n, q_s	Bed load transport in transverse and longitudinal direction, respectively
r, r_c	Local radius and radius at channel axis of channel curvature
\bar{u}, \bar{u}_{cr}	Mean and critical mean flow velocity
u, u_n, u_s	Maximum local flow velocity, split in its transverse and streamwise components
$u_*, u_{*,cr}$	Bed shear and critical bed shear velocity
$u_{s,z}$	Streamwise flow velocity per vertical coordinate z
z	Vertical coordinate over water column, positive downward
z_0	Roughness height
z_b	Local bed level
$\partial z_b / \partial n, \partial z_b / \partial s$	Transverse and longitudinal bed slope

Appendices

A Notes on samples of all sorting experiments

For most samples, notes were taken to describe the relief, small bed form types and/or the abundance of coarse grains. In Table A0, the different terms used in this appendix are explained. Terms that are self-explanatory, such as *fining upward* are excluded from this table.

Samples are organised per dune (two dunes were required for 1 sample) and per type of sample (top, trough, bulk), where "1" is congruous to the innermost sampled radius and "5" to the outermost sampled radius.

Table A0: Terms used in Appendix A1. Note that the words *coarse* and *fine* may be added to these terms to further describe these terms.

Term	Clarification
Coarse grains	Denotes the presence of coarse grains ($d_{50} > \pm 1$ mm) at the surface of the sample, using the following range: -- Coarse grains are present, but greatly outnumbered (<20) - Less than half the surface is covered with coarse grains + Fine grains can still be seen between the coarse grains ++ Entire surface is covered with coarse grains
Coarse ripple trough	Coarse grains are present in the ripple trough. Usually in the inner bend.
Drop crater	Small crater created by drops falling from the top lid after drainage. May mix grains within the top 1 cm. <i>Special case: downward drape sediment from drop crater:</i> sediment was transported from drop crater in inner bend toward the channel's axis. Was removed before sampling.
Dune rim	The highest point over the lateral that separated the dune (outer bend) from the ripples (inner bend). Made sampling a bit troublesome.
Ebb cap ripple	For scanning the bed level after an experiment had ended, very fine ripple brinkpoints became slightly flattened, resembling ebb caps found on dunes in tidal systems.
Fine top layer	Just below the surface, predominantly coarse grains were present, while the top was covered in relatively fine material.
Ripple relief	A collection of 3D bed form structures that made sampling troublesome. Occasionally sampling too deep (up to 1 cm).
Ripple rim	Same as ripple relief, but sampling was easier. May be both streamwise or transversely oriented.
Sheet ripple (edge)	Edge of very flat ripple, which is usually slightly coarser than the neighbouring grains. May slightly increase the coarse fraction in the sediment distribution.
Pebble cluster	Small agglomeration (< few cm) of grains that are slightly coarser than the neighbouring grains. These lay on top of the bed forms, looking like mini bed forms.

Table A1: Notes on samples of experiment 14 [$\theta = 0.065$ & $\partial z_b/\partial n = 0.26$]

		Notes dune 1	Notes dune 2
Top samples 1	1	ripple relief, ripple rim	—
	2	ripple relief	pebble cluster
	3	pebble cluster	pebble clusters
	4	—	—
	5	—	—
Top samples 2	1	ripple relief, ripple rim	ripple relief, ripple rim
	2	pebble cluster	—
	3	pebble cluster	pebble clusters
	4	—	—
	5	—	pebble clusters
Trough samples 1	1	pebble clusters	—
	2	downstream part sample coarser	pebble cluster
	3	fine top layer	coarse pebble cluster
	4	coarse sheet ripple	—
	5	—	—
Bulk samples	1	—	—
	2	—	—
	3	—	—
	4	—	—
	5	—	—

Table A2: Notes on samples of experiment 19 [$\theta = 0.142$ & $\partial z_b/\partial n = 0.04$]

		Notes dune 1	Notes dune 2
Top samples 1	1	ripple relief	ripple relief, pebble clusters
	2	–	pebble clusters
	3	3 drop craters, fine top layer	3 drop craters, edge sheet ripple, pebble clusters
	4	pebble cluster	edge sheet ripple, coarse grains (–)
	5	coarse grains (–)	>3 drop craters, slightly finer than sample 4
Top samples 2	1	ripple relief	pebble cluster
	2	ebb cap ripple, pebble clusters, coarse grains (–)	pebble clusters
	3	drop crater, pebble cluster	>3 drop craters, ebb cap ripple
	4	pebble clusters	edge sheet ripple, coarse grains (–)
	5	coarse grains (–)	drop craters, pebble cluster
Trough samples 1	1	coarse grains (–)	very fine compared to dune 1
	2	coarse grains (++)	upstream part sample coarse (++)
	3	drop crater, coarse grains (–)	drop crater, upstream part sample coarse (++)
	4	–	coarse grains (–)
	5	pebble clusters	coarse grains (–), finer in downstream dir.
Trough samples 2	1	2 drop craters, coarse grains (–)	
	2	coarse grains (++)	
	3	>3 drop craters	<i>not available</i>
	4	coarse grains (–)	
	5	coarse grains (–)	
Bulk samples	1	fining upward, lack of differentiation in upper part	
	2	fining upward, lack of differentiation in upper part	
	3	fining upward, lower 0.5 cm extremely coarse	
	4	–	
	5	–	

Table A3: Notes on samples of experiment 20 [$\theta = 0.065$ & $\partial z_b/\partial n = 0.01$]

	Notes dune 1	Notes dune 2
Top samples 1	1 drop crater, ebb cap ripple, coarse ripple trough	ripple relief, coarse grains (--)
	2 ripple relief, ebb cap ripple	ripple relief, ebb cap ripple, coarse ripple trough
	3 drop crater, ebb cap ripple, dune rim	drop crater, dune rim
	4 pebble cluster	coarse grains (-)
	5 coarse grains (-)	coarse grains (-), slightly coarser than dune 1
Top samples 2	1 ebb cap ripple, coarse ripple trough	ripple relief, ebb cap ripple, coarse ripple trough
	2 ebb cap ripple, coarse ripple trough	ripple relief, ebb cap ripple, coarse ripple trough
	3 dune rim	dune rim
	4 pebble cluster	coarse grains (--)
	5 coarse grains (++)	coarse grains (--)
Trough samples 1	1 ripple relief, ebb cap ripple, coarse ripple trough	ripple relief, ebb cap ripple, coarse ripple trough
	2 ripple relief, coarse grains (--)	ripple relief, ebb cap ripple, coarse ripple trough
	3 drop crater, ebb cap ripple, dune rim	pebble cluster
	4 pebble cluster	coarse grains (-), fine top layer
	5 drop crater, coarse grains (-), <i>accidentally sampled too deep</i>	coarse grains (--)
Trough samples 2	1 ebb cap ripple, coarse ripple trough	ripple relief, ebb cap ripple, medium coarse ripple trough
	2 2 ebb cap ripples, medium coarse ripple trough	ripple relief, 2 ebb cap ripples
	3 drop crater, pebble cluster	-
	4 coarse grains (--), sample coarser downstream	coarse grains (-)
	5 coarse grains (+)	coarse grains (+)
Bulk samples	1 difficult to determine lower boundary	
	2 difficult to determine lower boundary	
	3 possibly went to deep, so likely coarser	
	4 -	
	5 -	

Table A4: Notes on samples of experiment 21 [$\theta = 0.140$ & $\partial z_b / \partial n = 0.35$]

		Notes dune 1	Notes dune 2
	1	–	ripple rim
Top	2	edge sheet ripple fine, dune rim	ripple rim
samples 1	3	edge sheet ripple, fine pebble cluster	edge sheet ripple fine
<i>small dunes</i>	4	edge sheet ripple, fine pebble cluster, fine top layer	edge sheet ripple fine, coarse grains (––)
	5	coarse grains (–)	coarse grains (++)
	1	drop crater, medium coarse ripple trough, 2 ripple rims	medium coarse ripple trough, 2 ripple rims
Top	2	medium coarse ripple trough, ripple rim	ripple rim
samples 2	3	edge sheet ripple	edge sheet ripple
<i>large dunes</i>	4	edge sheet ripple	edge sheet ripple
	5	coarse grains (++)	coarse grains (++)
	1	–	downward drape sediment from drop crater
Trough	2	–	downward drape sediment from drop crater
samples 1	3	3 drop craters, coarse grains (––), fine top layer	pebble clusters
<i>small dunes</i>	4	coarse grains (––)	coarse grains (––)
	5	coarse grains (–)	coarse grains (++)
	1	–	coarse grains (+)
Trough	2	–	coarse grains (+)
samples 2	3	–	pebble clusters
<i>large dunes</i>	4	coarse grains (–)	coarse grains (–)
	5	drop crater, coarse grains (++)	coarse grains (––)
	1	–	
Bulk	2	–	
samples	3	–	
	4	–	
	5	–	

Table A5: Notes on samples of experiment 22 [$\theta = 0.107$ & $\partial z_b/\partial n = 0.22$]

		Notes dune 1	Notes dune 2
Top samples 1	1	ripple relief	ripple relief, pebble cluster
	2	edge sheet ripple	ripple relief
	3	–	edge sheet ripple
	4	edge sheet ripple, coarse grains (++)	edge sheet ripple fine, coarse grains (–)
	5	coarse grains (++)	coarse grains (++)
Top samples 2	1	drop crater, ripple relief	drop crater, ripple relief
	2	pebble cluster	dune rim, <i>accidentally dropped part sample</i>
	3	pebble clusters	–
	4	coarse grains (––), fine top layer	coarse grains (––)
	5	coarse grains (++)	coarse grains (++)
Trough samples 1	1	–	ripple rim
	2	coarse grains (––)	–
	3	coarse grains (++)	coarse grains (––)
	4	coarse grains (––)	coarse grains (–)
	5	coarse grains (–)	coarse grains (++)
Trough samples 2	1	pebble cluster	
	2	pebble clusters	
	3	coarse grains (––)	<i>not available</i>
	4	coarse grains (––)	
	5	drop crater, coarse grains (–)	
Bulk samples	1	–	
	2	–	
	3	–	
	4	–	
	5	–	

Table A6: Notes on samples of experiment 23 [$\theta = 0.064$ & $\partial z_b/\partial n = 0.26$]

		Notes dune 1	Notes dune 2
Top samples 1	1	2 ripple rims, medium coarse ripple trough	drop crater, ripple relief, ebb cap ripple
	2	drop crater, dune rim	ripple relief, medium coarse ripple trough, rim dune
	3	medium pebble cluster	sheet ripple, pebble cluster
	4	coarse grains (++)	coarse grains (++)
	5	coarse grains (++)	coarse grains (++)
Top samples 2	1	ripple relief, ebb cap ripple, medium coarse ripple trough	>3 drop craters
	2	edge sheet ripple, coarse pebble clusters	ripple relief, coarse pebble cluster
	3	edge sheet ripple, coarse pebble clusters	coarse grains (--)
	4	coarse grains (++)	coarse grains (++)
	5	coarse grains (++)	coarse grains (++)
Trough samples 1	1	ripple rim, pebble cluster	drop crater, ripple relief
	2	pebble cluster	coarse pebble clusters
	3	coarse grains (--)	coarse grains (--)
	4	coarse grains (++)	coarse grains (++)
	5	coarse grains (++)	coarse grains (-)
Bulk samples	1		
	2		
	3		
	4		
	5		

Table A7: Notes on samples of experiment 26 [$\theta = 0.098$ & $\partial z_b/\partial n = 0.05$]

		Notes dune 1	Notes dune 2
Top samples 1	1	ripple relief	>3 drop craters
	2	ripple rim	coarse pebble clusters, coarse grains (--)
	3	coarse pebble clusters	coarse pebble clusters, coarse grains (--)
	4	coarse grains (--)	coarse pebble clusters, coarse grains (--)
	5	>3 drop craters, coarse grains (--)	coarse pebble clusters, coarse grains (--)
Trough samples 1	1	3 drop craters, ripple relief	
	2	ripple relief, coarse pebble clusters	
	3	—	
	4	coarse grains (--)	
	5	coarse grains (--)	
Bulk samples	1	—	
	2	—	
	3	—	
	4	—	
	5	—	

Table A8: Notes on samples of experiment 27 [$\theta = 0.101$ & $\partial z_b / \partial n = 0.15$]

		Notes dune 1	Notes dune 2
Top samples 1	1	>3 drop craters, edge sheet ripple	ripple relief, edge sheet ripple, coarse pebble cluster
	2	edge sheet ripple, coarse pebble cluster	2 edge sheet ripples, dune rim
	3	edge sheet ripple	edge sheet ripple, coarse pebble cluster
	4	edge sheet ripple, coarse grains (--)	coarse pebble cluster, coarse grains (-)
	5	edge sheet ripple, coarse grains (--)	coarse grains (-)
Top samples 2	1	edge sheet ripple	ripple relief
	2	edge sheet ripple, dune rim	ripple relief
	3	edge sheet ripple	edge sheet ripple
	4	coarse grains (+)	edge sheet ripple, coarse grains (+)
	5	coarse grains (-)	edge sheet ripple, coarse grains (-)
Trough samples 1	1	ripple relief	ripple relief
	2	-	-
	3	-	coarse grains (++)
	4	coarse grains (--)	drop crater, coarse grains (--)
	5	coarse grains (++)	coarse grains (--)
Trough samples 2	1	>3 drop craters	>3 drop craters, dune rim
	2	-	2 edge sheet ripples
	3	dune rim	coarse grains (--), fine top layer
	4	coarse grains (--)	dune rim, coarse grains (-)
	5	coarse grains (--)	coarse grains (-), fine top layer
Bulk samples	1	-	
	2	-	
	3	-	
	4	-	
	5	-	

Table A9: Notes on samples of experiment 28 [$\theta = 0.057$ & $\partial z_b/\partial n = 0.18$]

		Notes dune 1	Notes dune 2
Top samples 1	1	drop crater, ripple relief	ripple relief
	2	ripple relief, dune rim	dune rim
	3	coarse grains (--)	coarse grains (--)
	4	coarse grains (++)	coarse grains (++)
	5	coarse grains (++)	coarse grains (++)
Top samples 2	1	ripple relief	>3 drop craters, ripple relief
	2	dune rim	pebble cluster
	3	<i>sample mistake - cannot be used</i>	pebble clusters, coarse grains (--)
	4	coarse grains (++)	coarse grains (++)
	5	coarse grains (++)	coarse grains (++)
Trough samples 1	1	—	ripple relief
	2	—	dune rim
	3	coarse grains (--)	coarse grains (--)
	4	coarse grains (--)	coarse grains (-)
	5	coarse grains (-)	coarse grains (++)
Trough samples 2	1	ripple relief	ripple relief, coarse grains (-)
	2	dune rim	ripple relief, dune rim
	3	<i>sample mistake - cannot be used</i>	edge sheet ripple
	4	coarse grains (-)	coarse grains (+)
	5	coarse grains (++)	coarse grains (+)
Bulk samples	1	—	
	2	—	
	3	—	
	4	—	
	5	—	

Table A10: Notes on samples of experiment 31 [$\theta = 0.078$ & $\partial z_b / \partial n = 0.23$]

		Notes dune 1	Notes dune 2
Top samples 1	1	drop crater, ripple relief, ebb cap ripple	drop crater, ripple relief
	2	ripple relief, dune rim	dune rim, coarse pebble cluster
	3	edge sheet ripple, dune rim	drop crater, edge sheet ripple, coarse pebble cluster
	4	coarse grains (--)	edge sheet ripple coarse, coarse grains (++)
	5	coarse grains (-)	coarse grains (++)
Top samples 2	1	drop crater, ripple relief, medium coarse ripple trough	drop crater, edge sheet ripple, coarse in ripple trough
	2	drop crater, ripple relief, medium coarse ripple trough, dune rim	dune rim
	3	coarse pebble clusters	drop crater, coarse pebble clusters
	4	coarse grains (++)	drop crater
	5	coarse grains (++)	coarse grains (++)
Trough samples 1	1	ripple relief, ebb cap ripple	dune rim
	2	coarse grains (--)	edge sheet ripple, coarse pebble cluster
	3	drop crater, coarse grains (--)	coarse grains (-)
	4	coarse grains (--)	coarse grains (++)
	5	coarse grains (-)	coarse grains (-)
Trough samples 2	1	2 drop craters, 2 ebb cap ripples	>3 drop craters
	2	ebb cap ripple	-
	3	-	coarse pebble cluster
	4	coarse grains (--)	drop crater, coarse grains (++)
	5	coarse grains (++)	coarse grains (++)
Bulk samples	1	-	
	2	-	
	3	-	
	4	-	
	5	-	

Table A11: Notes on samples of experiment 32 [$\theta = 0.091$ & $\partial z_b/\partial n = 0.07$]

		Notes dune 1	Notes dune 2
Top samples 1	1	ripple relief, medium coarse ripple trough	2 drop craters, ripple relief
	2	ripple relief, medium coarse ripple trough	ripple relief
	3	3 drop craters, dune rim, coarse pebble cluster	dune rim, coarse grains (--)
	4	coarse pebble clusters, coarse grains (++)	coarse grains (++)
	5	coarse grains (-)	coarse grains (++)
Top samples 2	1	drop crater, ripple relief, coarse ripple trough	>3 drop craters, ripple relief, medium coarse ripple trough
	2	coarse grains (-)	ripple relief, medium coarse ripple trough
	3	edge sheet ripple, dune rim	dune rim, coarse pebble cluster, coarse grains (--)
	4	2 edge sheet ripples, coarse pebble clusters	coarse grains (++)
	5	edge sheet ripple, coarse grains (-)	coarse grains (-)
Trough samples 1	1	>3 drop craters, ripple relief	2 drop craters, ripple relief
	2	dune rim, coarse grains (--)	ripple relief
	3	coarse grains (--)	coarse grains (-)
	4	coarse grains (++)	coarse grains (++)
	5	coarse grains (--)	coarse grains (++)
Trough samples 2	1	>3 drop craters, ripple relief	ripple relief
	2	ripple relief, medium coarse ripple trough	dune rim
	3	coarse grains (-)	coarse pebble cluster
	4	coarse grains (++)	coarse grains (-)
	5	coarse grains (++)	coarse grains (-)
Bulk samples	1		
	2		
	3		
	4		
	5		

Table A12: Notes on samples of experiment 33 [$\theta = 0.085$ & $\partial z_b / \partial n = 0.15$]

	Notes dune 1	Notes dune 2
Top samples 1	1 drop crater, ripple relief	>3 drop craters, ripple relief
	2 ripple relief, dune rim	dune rim
	3 coarse pebble clusters, coarse grains (--)	coarse pebble clusters
	4 edge sheet ripple coarse, coarse grains (++)	sheet ripple coarse, pebble clusters, coarse grains (--)
	5 coarse grains (++)	>3 drop craters, coarse grains (--)
Top samples 2	1 >3 drop craters, ripple relief, ebb cap ripple	ripple relief, coarse ripple trough
	2 coarse pebble cluster	ebb cap ripple, coarse grains (--)
	3 coarse pebble cluster	2 edge sheet ripples coarse
	4 coarse grains (++)	edge sheet ripple coarse, coarse grains (-)
	5 coarse grains (-)	coarse grains (--)
Trough samples 1	1 >3 drop craters, ripple relief, ebb cap ripple, coarse ripple trough	drop crater, ripple relief
	2 ripple relief, ebb cap ripple, medium coarse ripple trough	ripple relief, ebb cap ripple, coarse ripple trough
	3 coarse pebble clusters	coarse pebble clusters
	4 coarse grains (++)	coarse grains (++)
	5 coarse grains (++)	coarse grains (++)
Trough samples 2	1 ripple relief, coarse ripple trough	>3 drop craters, ripple relief
	2 drop crater, ripple relief	ripple relief, 2 ebb cap ripples
	3 coarse pebble clusters, coarse grains (--)	2 edge sheet ripples
	4 coarse grains (++)	coarse grains (-)
	5 coarse grains (-)	coarse grains (++)
Bulk samples	1	
	2	
	3	
	4	
	5	

Table A13: Notes on samples of experiment 34 [$\theta = 0.108$ & $\partial z_b/\partial n = 0.25$]

	Notes dune 1	Notes dune 2
Top samples 1	1 ripple relief, ebb cap ripple	ripple relief, medium coarse ripple trough
	2 complex ripple, coarse ripple trough, pebble clusters	ripple rim, medium coarse ripple trough
	3 pebble cluster, coarse grains (--)	edge sheet ripple, pebble clusters
	4 coarse grains (-)	coarse grains (-)
	5 coarse grains (-)	coarse grains (++)
Top samples 2	1 -	2 drop craters, ripple relief
	2 ripple relief, medium coarse ripple trough	coarse grains (--)
	3 ebb cap ripple	edge sheet ripple, pebble cluster, coarse grains (--)
	4 coarse grains (++)	edge sheet ripple, coarse grains (++)
	5 coarse grains (++)	coarse grains (++)
Trough samples 1	1 drop crater, ripple rim	ripple relief
	2 pebble cluster, coarse grains (--)	ripple relief, pebble cluster
	3 -	pebble clusters, coarse grains (-)
	4 (++)	coarse grains (++)
	5 coarse grains (++)	coarse grains (++)
Trough samples 2	1 -	drop crater, ripple relief
	2 pebble clusters	ripple rim, pebble clusters
	3 coarse grains (-)	coarse grains (--)
	4 coarse grains (-)	coarse grains (-)
	5 coarse grains (-)	coarse grains (-)
Bulk samples	1 -	
	2 -	
	3 -	
	4 -	
	5 -	